AN ABSTRACT OF THE THESIS OF

S. Morgaine McKibben for the degree of Master of Science in Oceanography
presented on September 2, 2011.

Title: Development of Satellite Bloom Detection Products for Coastal Oregon

Abstract approved:

_____

Angelicque E. White

Two bloom-detection products were developed for the Oregon coast that describe the relative percent change observed between successive pairs of 8-day chlorophyll-a (CHL) and fluorescence line-height (FLH) products obtained from the MODerate Resolution Imaging Spectroradiometer aboard the Aqua spacecraft (MODIS-Aqua). The CHL_{dev} and FLH_{dev} products, respectively, were optimized to detect bloom onset via satellite in a region typified by high-frequency biological variability at the time scale of days and persistent cloud cover. Daily CHL_{dev} and FLH_{dev} imagery highlights the geographic locations of greatest temporal change observed between weekly average CHL or FLH products over time, providing a way to track the onset and advection of algal blooms. "Bloom indices" based on CHL_{dev} and FLH_{dev} were developed as a temporal metric of regional-scale bloom events. Comparison of these indices to *in situ* mooring data collected off the central Oregon coast from summer 2009 through winter 2010 demonstrated successful detection of all upwelling-induced bloom events, plus a late-season harmful algal bloom associated with wind relaxation and warming surface waters. During summer and autumn of 2009, significant correlation was observed between blooms detected by the CHL_{dev} and FLH_{dev} indices and two *in situ* metrics of upwelling-favorable conditions: 1)

temperature, with temporal lags of -1 (r=-0.41) and 0 days (r=-0.45), respectively, and wind stress, with temporal lags of +2 (r=-0.25 and -0.41, respectively). Consistent with the regional oceanography, winds were shown to be dominant drivers of observed blooms during the summer and autumn. Winter 2009 through spring 2010 yielded high-variability bloom indices, due to frequent, variable cloud coverage, and no significant correlation was observed between the indices and *in situ* data. Coupled with physical proxies collected via satellite or *in situ,* these products provide an excellent foundation for remote bloom detection in Oregon's coastal waters and regions with similar biological and physical conditions.

Development of Satellite Bloom Detection Products for Coastal Oregon

by
S. Morgaine McKibben

A THESIS

submitted to

Oregon State University

in partial fulfillment of
the requirements for the
degree of

Master of Science

Presented September 2, 2011
Commencement June 2012

Master of Science thesis of S. Morgaine McKibben presented on September 2, 2011

APPROVED:

_____

Major Professor, representing Oceanography

_____

Dean of the College of Oceanic and Atmospheric Sciences

_____

Dean of the Graduate School

I understand that my thesis will become part of the permanent collection of Oregon State University libraries. My signature below authorizes release of my thesis to any reader upon request.

_____

S. Morgaine McKibben, Author

ACKNOWLEDGMENTS

I thank:

Dr. Angelicque White for your guidance, time, and confidence in me and for exemplifying a standard to strive for. Dr. Peter Strutton for starting my graduate career by taking me on as graduate student and providing excellent guidance and support during my first year.

The grants and fellowship that supported my research and provided an excellent opportunity for me to learn and develop my skills as a researcher: NOAA grant NA07NOS4780195 from the Monitoring and Event Response for Harmful Algal Blooms (MERHAB) program; NA08NES4400013 to the Cooperative Institute for Oceanographic Satellite Studies; funding from the Center for Coastal Margin Observation and Prediction (CMOP); and the Diversity Advancement Pipeline Fellowship (2009-2010 academic year).

The wonderful people of the Letelier/White/Davis lab that have helped along the way by answering my questions, helping troubleshoot problems, giving input on practice talks and providing excellent feedback and advice in general. I feel lucky to work with such a helpful, supportive and fun group of people.

Last, but far from least, my mom for teaching me to, above all else, live life passionately and follow my bliss. And my wonderful husband Chris for a partnership that is an infinite source of happiness, fun, togetherness and stability. Thank you for always being there to celebrate the good times, support me through the bad, and for believing in and encouraging me every step of the way.

CONTRIBUTION OF AUTHORS

Angelicque White provided design and intellectual contributions as well as editing for material presented in Chapter 2. Pete Strutton provided intellectual contributions to the original research design and material presented in Chapter 2. Dave Foley provided intellectual contributions and initial code design for Chapter 2. Tawnya Peterson provided intellectual contributions for the material presented in Chapter 2. Each of the aforementioned are co-authors for the submitted or accepted manuscripts of these respective chapters.

TABLE OF CONTENTS

TABLE OF CONTENTS (Continued)

LIST OF FIGURES

LIST OF FIGURES (Continued)

1. PHYTOPLANKTON DYNAMICS AND SATELLITE REMOTE SENSING

1.1 Introduction

1.1.1 Phytoplankton and chlorophyll-a

Phytoplankton are a sentinel class of organisms in the marine environment. These microscopic primary producers convert dissolved inorganic carbon into particulate organic matter that sustains the marine food web, making them indicators of both the biological productivity of the system and the amount of carbon it assimilates over time. Driven by physical and chemical processes including changes in wind, temperature, light and nutrient concentrations, the abundance and distribution of phytoplankton can elucidate a region's particular environmental forcing. They are also indicators of anthropogenic influences on marine systems, for example, intense coastal blooms induced by eutrophication. As a result of these combined factors, quantification of how phytoplankton biomass varies over time serves as a foundation for understanding biological processes in the upper ocean.

Phytoplankton can be prokaryotic or eukaryotic and vary over orders of magnitude in size, have highly varied physiology and use an array of pigments to harvest light energy from the sun to fuel photosynthesis; however, nearly all possess the pigment chlorophyll-a (chl-a) which exhibits signature wavelengths of absorption and emission (fluorescence) in the visible spectrum. Chl-a is ubiquitous among phytoplankton and its optical properties are relatively easy to quantify. As such, chl-a concentration is an ideal proxy for biomass and hence comprises the basis of many optical techniques used to quantify bulk phytoplankton standing stock. Intriguingly, the signature absorbance and emission spectra of chl-a also gives us the power to quantify these microscopic organisms from space at a global scale.

1.1.2 Satellite ocean color sensors

Ocean color sensors aboard Earth-orbiting satellites are now central tools in oceanographic research, providing a synoptic view of chl-a concentrations for nearly the entire ocean domain each day. The successful 1978 launch and subsequent implementation of the Coastal Zone Color Scanner (CZCS) marked the inception of satellite ocean color research. This one-year proof-of-concept mission, which ultimately remained in service until 1986, demonstrated chl-a concentration could be remotely measured via satellite (Hovis et al. 1980). Several successors to CZCS have since been launched, including the Sea-viewing Wide Field-of-view Sensor (SeaWiFS) (Hooker & Esaias 1993) and the Moderate-resolution Imaging Spectroradiometers (MODIS-Aqua and MODIS-Terra) (Ardanuy et al. 1991). All of these instruments use bio-optical algorithms to derive geophysical parameters, such as chl-a concentration, from water-leaving radiance, or light scattered from the ocean's surface (O'Reilly et al. 1998). With these data, the abundance and distribution of phytoplankton can be estimated at regional and global scales that could never be achieved by *in situ* methods alone.

1.1.3 Bloom dynamics

Phytoplankton blooms, or rapid increases in biomass, are sensitive biophysical indicators of marine ecosystems. As such, methods of bloom detection based on proxies of chl-a variability are fundamental to the study of phytoplankton bloom dynamics. Coupled with ancillary biological and physical data, bloom proxies can yield important insights into the conditions that induce blooms, as well as how they affect the ecology or chemistry of the marine environment. For example, coincident physical parameters, such as temperature, salinity, wind stress and nutrient concentrations, can be used to determine what conditions are associated with bloom initiation. Alternatively, if biological response following a bloom is of interest, coincident *in situ* quantification of consumers is necessary.

In addition to ancillary data, consideration of spatio-temporal variability inherent in the system of study is another critical component of researching bloom dynamics. The marine environment is a vast, three-dimensional environment that is highly variable in time and space, making sampling efforts and subsequent interpretation of data challenging. For instance, blooms are often mesoscale (10's-100's of km) phenomena that occur over a wide range of time scales, from hours to weeks or more, but shipboard measures of phytoplankton biomass describe small points in space and time and can be difficult to extrapolate to larger scales. Autonomous platforms, such as moorings, offer much longer time series, but are also limited in spatial coverage. In contrast, satellite ocean color data describe mesoscale phytoplankton abundance across a majority of the world's surface oceans each day, however they lack the detail of *in situ* measures, such as community composition or subsurface distribution patterns. Considering the complementary strengths and weaknesses of satellite and *in situ* data in terms of coverage, merging of the two provides an ideal foundation to study regional bloom dynamics through more accurate interpretation of each.

1.1.4 Thesis objectives

The primary goal of this research is to develop customized bloom-detection products for the Oregon coast based on relative changes in satellite ocean color data over time. The products were designed to identify and track phytoplankton blooms according to this region's high spatio-temporal variability in phytoplankton growth and frequency of persistent cloud cover, which inhibits collection of satellite data. Following development, products were assessed against one year of *in situ* data from the central Oregon coast to evaluate 1) their efficacy in terms of accurately detecting bloom events and 2) their utility in identifying dominant physical drivers of the observed events.

1.1.5 Literature cited

Ardanuy PE, Han D, Salomonson VV (1991) The Moderate Resolution Imaging Spectrometer (MODIS) science and data system requirements. Geoscience and Remote Sensing 29:75-88

Hooker S, Esaias W (1993) An overview of the SeaWiFS project. EOS Transactions 74:241-241

Hovis W, Clark D, Anderson F, Austin R, Wilson W, Baker E, Ball D, Gordon H, Mueller J, El-Sayed S (1980) Nimbus-7 Coastal Zone Color Scanner: system description and initial imagery. Science 210:60

O'Reilly JE, Maritorena S, Mitchell BG, Siegel DA, Carder KL, Garver SA, Kahru M, McClain C (1998) Ocean color chlorophyll algorithms for SeaWiFS. Journal of Geophysical Research 103:24937

Development of satellite bloom detection products for coastal Oregon

Morgaine McKibben[1], Peter G. Strutton[2], Dave Foley[3], Tawnya Peterson[4] and Angelicque E. White[1]*

[1]Oregon State University, College of Oceanic and Atmospheric Sciences, Corvallis, Oregon, USA

[2]Institute for Marine and Antarctic Studies, University of Tasmania, Hobart, Tasmania, Australia

[3]NOAA Southwest Fisheries Science Center, Environmental Research Division, Pacific Grove, California, USA

[4]Oregon Health and Science University, Division of Environmental and Biomolecular Sciences, Beaverton, OR, USA

*Corresponding author e-mail: morgaine@coas.oregonstate.edu

In preparation for submission to Marine Ecology Progress Series

International Ecology Institute

Nordbunte 23 (+3,5,28,30) 21385 Oldendorf/Luhe Germany

2. DEVELOPMENT OF SATELLITE BLOOM DETECTION PRODUCTS FOR COASTAL OREGON

2.1 Abstract

Two bloom-detection products were developed for the Oregon coast that describe the relative percent change observed between successive pairs of 8-day chlorophyll-a (CHL) and fluorescence line-height (FLH) products obtained from the MODerate Resolution Imaging Spectroradiometer aboard the Aqua spacecraft (MODIS-Aqua). The CHL_{dev} and FLH_{dev} products, respectively, were optimized to detect bloom onset via satellite in a region typified by high-frequency biological variability at the time scale of days and persistent cloud cover. Daily CHL_{dev} and FLH_{dev} imagery highlights the geographic locations of greatest temporal change observed between weekly average CHL or FLH products over time, providing a way to track the onset and advection of algal blooms. "Bloom indices" based on CHL_{dev} and FLH_{dev} were developed as a temporal metric of regional-scale bloom events. Comparison of these indices to *in situ* mooring data collected off the central Oregon coast from summer 2009 through winter 2010 demonstrated successful detection of all upwelling-induced bloom events, plus a late-season harmful algal bloom associated with wind relaxation and warming surface waters. During summer and autumn of 2009, significant correlation was observed between blooms detected by the CHL_{dev} and FLH_{dev} indices and two *in situ* metrics of upwelling-favorable conditions: 1) temperature, with temporal lags of -1 (r=-0.41) and 0 days (r=-0.45), respectively, and wind stress, with temporal lags of +2 (r=-0.25 and -0.41, respectively). Consistent with the regional oceanography, winds were shown to be dominant drivers of observed blooms during the summer and autumn. Winter 2009 through spring 2010 yielded high-variability bloom indices, due to frequent, variable cloud coverage, and no significant correlation was observed between the indices and *in situ* data. Coupled with physical proxies collected via satellite or *in situ,* these products provide an excellent foundation for remote bloom detection in Oregon's coastal waters and regions with similar biological and physical conditions.

KEY WORDS: Oregon coast · California Current · Upwelling · Bloom timing · Phenology

ACKNOWLEDGEMENTS: . Gratitude is expressed to Dr. Stephen Pierce and Dr. Wiley Evans for data provided. This study was supported by NOAA grant NA07NOS4780195 from the Monitoring and Event Response for Harmful Algal Blooms (MERHAB) program and NA08NES4400013 to the Cooperative Institute for Oceanographic Satellite Studies. The statements, findings, conclusions, and recommendations are those of the author(s) and do not necessarily reflect the views of the National Oceanic and Atmospheric Administration or the Department of Commerce. This is MERHAB publication no, xx.

2.2 Introduction

Phytoplankton are fundamental to the export of carbon from surface seawater to the deep ocean, hence they regulate climate, are integral to elemental cycling in the global ocean, are necessary to sustain ecosystem productivity and serve as reservoirs of energy, elements and genetic diversity. Given these functions, considerable resources have been devoted to understanding the temporal and spatial variability of phytoplankton biomass and productivity, which are tightly coupled with the physical environment. When temperature, light and nutrient conditions are favorable, phytoplankton populations experience a rapid increase in abundance, the classic hallmark of a “bloom.” As such, the study of phytoplankton bloom dynamics is a fundamental component of characterizing the critical roles that phytoplankton play in marine ecosystems and biogeochemical cycles. In this context, bloom dynamics include the physical conditions that induce bloom onset, the biological and physical mechanisms that affect bloom duration and to what extent blooms affect the ecology and chemistry of the marine environment**.**

Since the initial Coastal Zone Color Scanner (CZCS) experiment in 1978, ocean color has been used to quantify the concentration of phytoplankton from space, providing researchers with a powerful tool to study mesoscale bloom dynamics (10s to

100s of kilometers). Satellite chlorophyll-a (chl-a) measurement relies on spectral changes in water leaving radiance, the radiance backscattered upward from the ocean's surface (O'Reilly et al. 1998). Chl-a is ubiquitous among phytoplankton as means to absorb solar energy for photosynthesis; excess energy not used for photosynthesis is dissipated as heat or emitted as fluorescence. Based on this premise, two coincident ocean color products from the MODerate resolution Imaging Spectroradiometer aboard the Aqua spacecraft (MODIS-Aqua) estimate phytoplankton biomass and physiology from space: chl-a concentration (CHL) and fluorescence line height (FLH), respectively. The empirical algorithm used to derive CHL is a polynomial best-fit between ground-truthed *in situ* chl-a concentrations and satellite-observed radiances (Werdell & Bailey 2005) that indirectly measures solar radiation absorbed by chl-a in the surface ocean. FLH is a line-height algorithm based on the spectral shape of water-leaving radiance in the red, as determined by solar-stimulated fluorescence emission by chl-a (Letelier & Abbott 1996).

Tracking changes in CHL and FLH over time has informed studies of the response of phytoplankton to climate change (Behrenfeld et al. 2006), shifts in physiology in response to trace metal limitation (Behrenfeld et al. 2009) and the potentially confounding role of colored dissolved organic matter (CDOM) in estimating chl-a via satellite (Siegel et al. 2005a), to name a few applications. In concert with *in situ* data, the relative change of CHL and FLH provide a tracer for phytoplankton blooms and physical transport of phytoplankton biomass, which can inform sampling and monitoring efforts. For example, a chl-a anomaly product developed for the west Florida shelf is used to monitor blooms of *Karenia brevis*, a toxic dinoflagellate. The product highlights regions with the greatest increase in bulk chl-a concentration relative to a climatalogical average. With *in situ* sampling, modeling, meteorological and oceanographic mooring data, this product is successfully used to identify and track potential *Karenia brevis* blooms (Stumpf 2001).

Blooms are typically defined as a rapid increase of algal biomass over time among one, or a small number of, phytoplankton species (Smayda 1997b). Beyond this generalized definition, the quantitative metric of a bloom is subjective, varying among research efforts according to region and time frame of study, as well as application of *in situ* versus satellite methods of phytoplankton quantification. For example, the satellite product for the west Florida shelf defines bloom initiation as a 1 mg m^{-3} or greater increase in chl-a concentration for a single day relative to the previous 60 day average with a 15-day lag between the two (Stumpf 2001). Other studies have used similar threshold approaches, such as defining blooms based on deviation from a median or a static value (Siegel et al. 2002a, Wilson 2003, Henson & Thomas 2007a). The need to establish universal bloom criteria has been expressed, and potential methods proposed (e.g. Smayda 1997a, b, Mieruch et al. 2010), but blooms represent a complex biological response to a variety of natural and anthropogenic conditions that vary according to region, community composition and time of year. These factors, among others, complicate attempts to develop a unilateral set of bloom definitions.

Blooms are a cornerstone of productive coastal upwelling regimes, hence are critical to the vitality of the ecosystems and local economies that depend on them. For example, Oregon's coastal waters reside in the northern portion of the California Current System (CCS), a productive eastern-boundary upwelling regime. Throughout the upwelling season (roughly May through September, depending on year), the region's bloom dynamics have far-reaching effects, from fueling a rich and diverse food web and associated fisheries harvests (Ware & Thomson 1991, 2005) to driving rapid fluctuations in the air-sea flux of carbon dioxide (Evans et al. 2011). Blooms also affect the severity and spatial extent of hypoxic zones induced by bloom decomposition in pre-conditioned low-oxygen waters near the seafloor (Grantham et al. 2004). Additionally, a subset of blooms are composed of primarily toxigenic, or otherwise harmful, species of algae and are a regular seasonal phenomenon in Oregon waters (Trainer et al. 2010, Tweddle et al. 2010). These harmful algal blooms (HABs)

can cause mass mortality of marine animals (Phillips et al. 2011) or threaten human health through consumption of toxic shellfish (Trainer et al. 2010). Phytoplankton blooms are a fundamental driving force in all of the above, underscoring the need for satellite-based bloom products which afford the ability remotely identify and track blooms at the mesoscale level. However, the region is characterized by frequent cloud cover, which limits satellite coverage, and high spatial and inter-annual variability in phytoplankton biomass where the magnitude of annual maximal in-water chl-a varies by a factor of 2 or greater, complicating efforts to define a static threshold for blooms. In this regard, we have designed products optimized for the spatial and temporal variability inherent to Oregon's coastal waters that detect changes in surface chl-a concentration over time.

2.2.1 Development of bloom products for the Oregon coast

CHL and FLH are both functions surface chl-a concentrations, making them ideal foundations for Oregon coast bloom detection products. However, CHL accuracy is known to decline in coastal environments because the *in situ* dataset used to parameterize the CHL algorithm consists of samples predominantly from clear open-ocean, or Case 1, waters. Comparatively optically-complex Case 2 waters are not well represented, introducing error into CHL retrievals in these regimes (Werdell et al. 2007, Claustre 2003). Additionally, the CHL algorithm cannot differentiate between chl-a and colored dissolved organic matter (CDOM) as both absorb light strongly in the blue region of the visible spectrum, leading to overestimates of CHL in waters with elevated CDOM concentrations (Claustre 2003, Siegel et al. 2005b). River discharge is a distinctive feature of the Oregon coast (Hickey et al. 2005, Wetz et al. 2006) and a prominent regional-scale control on satellite-derived distributions of CDOM (Siegel et al. 2002b) suggesting CHL values in this region may be over-estimated during periods, or at sites, of high riverine outflow. In contrast, the FLH algorithm lacks bias from an *in situ* dataset (Letelier & Abbott 1996) and CDOM has been shown to not affect FLH measurements (Hoge et al. 2003). Chl-a fluorescence

has long been used as a proxy of phytoplankton biomass in biological oceanography (Kiefer & Reynolds 1992) and FLH is commonly applied as such as well (Letelier & Abbott 1996, Behrenfeld et al. 2009); however, FLH is actually a complicated function of both biomass and phytoplankton physiology that varies according to algal assemblage composition, temperature, light and nutrient availability (Letelier & Abbott 1996). As such, fluorescence is also source of physiological information (Kiefer & Reynolds 1992, Behrenfeld et al. 2009) and select studies have explored application of FLH as a physiological indicator (e.g. Behrenfeld et al. 2009).

Considering the influence of CDOM on CHL and physiology on FLH, both were used to develop coincident bloom products with the intent of comparing and contrasting output of the two to better evaluate resultant bloom signals. To a first order, CHL, FLH, as well as the bloom products based on them, will be considered proxies of chl-a concentration throughout development and initial assessments of performance. To evaluate this assumption, we have compared satellite CHL and FLH to *in situ* data. Subsequent discussion of product output will include similarities and differences observed between bloom product output and potential causes, including the impact of CDOM and physiology on CHL and FLH.

2.2.2 Coupled biological-physical dynamics of Oregon's coastal waters

The observed seasonal and intra-seasonal dynamics of wind stress, river discharge and biology guided development of the algorithm used to derive both bloom products. Variability in wind stress and river discharge are dominant drivers of biological variability in Oregon's coastal waters. Throughout late spring, summer and early autumn, blooms are induced by upwelling-favorable winds that drive Ekman transport of water offshore, bringing cold, nutrient-rich water to the surface. Upwelling events and subsequent blooms are punctuated by reversals or relaxations in wind stress at periods of approximately 20 days (Bane et al. 2007), hence typical summer conditions can be described as "upwelling-favorable with a downwelling event a few days in the past" (Banas et al., 2009). In contrast, winter and early spring

are characterized by alternation between periods of high-magnitude downwelling-favorable winds and relaxation events coupled with low productivity relative to the upwelling season.

Wind stress variability also strongly influences the location of the Columbia River plume (Hickey et al. 2005), the largest source of freshwater discharge into the Pacific Northwest (Naik & Jay 2005). In summer and early autumn the plume shifts southward from the Columbia River mouth towards Oregon in two general 'modes' relative to the coastline: close to shore when downwelling-favorable winds induce bi-directional alongshore transport of the plume towards both Washington and Oregon, or offshore when winds are upwelling-favorable (Hickey et al. 2005). The plume represents a considerable influx of freshwater rich in macro- and micronutrients, suspended particles and organic matter into the marine environment. As such, it can stimulate or suppress productivity by altering nutrient concentrations, water column stratification, light levels and circulation (Banas et al. 2009, Kudela et al. 2010).

During winter and spring the plume shifts predominately northwards (Hickey et al. 2005), and numerous smaller coastal rivers flowing from the Coast Range become the region's primary source of riverine discharge and a potentially dominant driver of primary productivity (Wetz et al. 2006). Outflow from these rivers peaks from roughly November through April during which time winter storms bring punctuated periods of high rainfall and snowmelt in the spring (Wetz et al., 2006). The nutrients supplied by these rivers may stimulate winter primary productivity, an under-studied occurrence estimated to represent approximately 20% of the productivity that occurs during summer upwelling conditions (Wetz et al., 2006). At their wintertime peak flow levels, rivers draining into in the northern CCS (40.5º N to the northern Washington border) collectively have a coastline-normalized discharge rate 52-97% greater than the rates of all other major eastern-boundary current systems (Wetz et al., 2006), underscoring the potential significance of biological and physical effects induced by wintertime river discharge in this region.

The overarching goal of this research is to develop customized satellite products for the Oregon coast that provide a metric of variability in terms of onset, advection and decay of blooms. The aforementioned patterns in the region's wind stress variability and river outflow, limitations of satellite coverage and desired research applications guiding product development and will be described herein. First, we will evaluate the relative accuracy and coverage of ocean color data in the region as well as the temporal scale of *in situ* chl-a records as a metric of biological variability. Observed scales of variability and frequency of satellite coverage will be used to determine the parameters of the bloom product algorithm. The algorithm will be applied to standard CHL and FLH datasets to create two separate bloom products, CHL_{dev} and FLH_{dev}. Coincident *in situ* biological and physical data from the central Oregon coast will then be used to evaluate product performance in terms of accurate detection of bloom events and identification of the dominant physical drivers of the observed events.

2.3 Methods

2.3.1 Study area

The bloom products were developed and optimized for the coastal waters of Oregon and southern Washington, defined here as 42ºN to 47ºN and 0.5º latitude west of the coastline. To examine coast-wide trends, satellite data were binned into five regions, A through E, 1º of latitude by 0.5º longitude in size (Figure 2-1a). Bin size was based on observed patterns in latitudinal CHL variability induced by north-south gradients in wind stress, solar insolation and bathymetry (Henson & Thomas 2007b, Venegas et al. 2008, Tweddle et al. 2010) and focuses on waters over the continental shelf where CHL is greatest (Henson & Thomas 2007a, Venegas et al. 2008). Product performance was evaluated in region C, which coincides with location of available *in situ* mooring data at NH-10, a hydrographic station located 10 miles offshore of Newport, Oregon at 44.6ºN and 124.3ºW (Figure 2-1a).

2.3.2 In situ *data*

Time series of fluorescence, salinity and temperature data collected at the NH-10 mooring were obtained as metrics of in-water biological and physical parameters. Fluorescence was measured by a Wet Labs Combination Fluorometer and Turbidity Sensor (ECO- FLNTUSB) mounted approximately one meter below the surface. Raw fluorescence counts were obtained once per second for five seconds each hour. No efforts were made to convert raw data to calibrated units. Available fluorescence data span August through December 2007, April through August 2009 and March through May 2009. The intervals are somewhat aperiodic due to variability in instrument performance (bio-fouling) and weather, which limited servicing and deployment opportunities. Temperature and salinity data spanning April 2009 through May of 2010 from the NH-10 mooring were also obtained. This time frame was chosen as it represented the most continuous available temperature and salinity records spanning a full year. Measurements were taken every 10 minutes at 2 meters below the surface. All time series data averaged to yield daily intervals.

Coastal river discharge and wind stress data were obtained to explore their relation to observed blooms. Raw wind data from the National Data Buoy Center's NWPO3 station at Newport, Oregon (Figure 2-1a) was used to derive daily wind stress for the central Oregon coast using the method of Large and Pond (1981). Streamflow records were acquired as a metric of river discharge from the United States Geological Survey for 2005-2010 (http://waterdata.usgs.gov/nwis/sw). Daily mean streamflow values were obtained for all USGS-gauged rivers west of the Coast Range at the furthest downstream gauging station available (Figure 2-1a). Regions B-D each include two to three rivers with headwaters in the Coast Range that drain into the Pacific, while region E has one. Region A includes only the Columbia River, and Region E also includes two coastal rivers that empty into the Pacific but represent a watershed just south of the Coast Range. The median daily discharge from all rivers within each region was calculated as a measure of freshwater input using the previously described latitudinal bounds.

2.3.3 Satellite data

Co-located CHL and FLH data from MODIS-Aqua comprise the foundation of the two bloom products. All swaths, or data obtained from a single satellite pass, spanning 2005-2010 and containing viable data in the northeastern Pacific Ocean region (134ºW to 121ºW and 52ºN to 34ºN) were obtained from the Ocean Biology Processing Group (OBPG; http://oceancolor.nasa.gov) as Level-2 (L2) hierarchical data format (HDF) files (processing version R2009.1, created by l2gen version 6.2.5). L2 HDF files include standard geophysical variables, such as CHL and FLH, as well as OBPG-defined flags used for quality-control of data. Level-3 (L3) mapped products were created by extracting data for each geophysical variable of interest from the L2 HDF file then masking the data according to the following standard NASA quality-control flags: 1, atmospheric correction failure; 2, pixel is over land; 5, observed radiance very high or saturated; 10, cloud or ice contamination; and 26, navigation failure. Next, masked data were mapped to an equal-area 1-kilometer (km) standard grid to yield L3 swath data, which were then temporally-binned into daily files using arithmetic composite-averaging. L2 to L3 processing was identical for both ocean color products, yielding two datasets of daily L3 CHL and FLH at 1-km resolution spanning 2005-2010.

The primary sources of error in these products include performance of the CHL and FLH algorithms in this region, atmospheric correction methods applied during L2 processing, the presence of CDOM, sensor accuracy and calibration, solar zenith angle at time of satellite flyover, physiological variability of phytoplankton assemblages and selective application of quality-control flags during L3 processing**.** Considering these error sources, a baseline assessment of CHL and FLH accuracy in this region would optimize interpretation of the bloom products. As we are not aware of any previous validation efforts in Oregon's coastal waters, linear regression analysis of daily CHL and FLH retrievals and *in situ* fluorescence at NH-10 was employed as first order approximation of satellite data accuracy for the region. Daily mean CHL and FLH values were approximated by averaging values over a 3 pixel by

3 pixel (3 km by 3 km) box centered over the NH-10 mooring and regressed against daily average raw counts obtained from the mooring's fluorometer for the corresponding day. Primary sources of error in the regressions include the errors mentioned above, chl-a concentrations at the time of satellite flyover relative to average conditions measured throughout the day *in situ*, spatial averaging of retrievals across a 9 km^2 area and biofouling of the fluorometer.

Two satellite images describing physical conditions were obtained to aid interpretation of the bloom products in case studies described in the discussion. Standard MODIS L3 8-day 4-km resolution sea surface temperature (SST) imagery was obtained for February 15-22, 2006 from the OBPG as a metric of potential freshwater outflow, which typically appears as regions of warmer temperatures. Sea surface height (SSH) imagery from Archiving, Validation and Interpretation of Satellite Oceanographic data (AVISO) was obtained for September 26, 2009 (http://las.pfeg.noaa.gov/oceanWatch/oceanwatch.php). The data are 0.25º (~28 km) resolution and were used to add contour intervals as descriptors of SSH anomalies coincident with bloom imagery.

2.3.4 Bloom product algorithm

Satellite coverage, which is predominantly a function of the frequent cloud cover in this region, was a primary consideration in algorithm development. Clouds block the sensor's view of the ocean surface, resulting in negative, or invalid, retrievals. In this region it is not uncommon for time series trends in daily ocean color data to yield too few pixels each day to discern any meaningful patterns in chl-a concentration. As a result, iterative, or "running," composite-averaging was applied to daily standard CHL and FLH products over 8-day periods (see below and discussion for determination of this time frame) in order to attain a greater number of positive, or valid, retrievals across the spatial domain of interest. For each day, running 8-day composites yield imagery comprised of data averaged across that day and the previous

seven days. Daily relative differences between 8-day CHL or FLH composites comprise the foundation of the bloom product algorithm (Equation 1).

$$X_{dev} = \frac{\overline{X}_{current} - \overline{X}_{reference}}{\overline{X}_{reference}} \times 100\% \qquad \text{(Equation 1)}$$

Where X_{dev} is the pixel value of either CHL or FLH at a specific location derived from the relative difference between the pixel values at the same location in the two running composites, $\overline{X}_{current}$ and $\overline{X}_{reference}$, and is repeated for each pixel in the defined coordinate plane. Daily CHL and FLH products were composite-averaged to calculate $\overline{X}_{current}$ and $\overline{X}_{reference}$ for each product, yielding $\overline{C}_{current}$, $\overline{C}_{reference}$ and $\overline{F}_{current}$, $\overline{F}_{reference}$, respectively. In this region, CHL exhibits lognormal distribution over time and space and FLH exhibits a normal distribution, warranting different composite-averaging methods for each product. The geometric mean was applied to calculate $\overline{C}_{current}$ and $\overline{C}_{reference}$ and the arithmetic mean was used to calculate $\overline{F}_{current}$ and $\overline{F}_{reference}$. Note the paired composites represent successive 8-day periods and do not overlap in time. Application of this algorithm to 8-day CHL or FLH datasets yields the bloom products CHL_{dev} and FLH_{dev}, respectively.

Biological variability in this region is driven by rapidly-changing physical dynamics, yet satellite coverage is significantly hampered by cloud cover. This suggests the number of days across which the current and reference composites are averaged needs to be as small as possible to capture variability in surface chl-a concentration at scales of a few days, yet large enough to provide a sufficient number of positive satellite retrievals to produce meaningful results. Two factors were evaluated to determine appropriate time frames for the composites: observed temporal scales of *in situ* biological variability and the frequency of satellite coverage at NH-10. First, scales of biological variability were assessed through auto-correlation analysis of all three NH-10 *in situ* fluorescence datasets.

Second, the percent of positive retrievals achieved by the daily products was assessed for the 2005-2010 CHL dataset in two ways: 1) determination of the average gap observed between positive, or valid, retrievals at NH-10 and 2) a spatial map

describing average percentage of positive retrievals achieved in L3 daily CHL. To quantify gaps in coverage, daily CHL data were obtained from the pixel coincident with NH-10 for 2005-2010 and assigned a value of one or zero to indicate whether a positive or negative retrieval, respectively, was obtained for that day. Gap length was determined by summing the total number of consecutive negative retrievals between each positive retrieval, then the average gap length, standard deviation, median and mode were calculated. The geographical coverage of daily L3 CHL products was also quantified by assigning values of one and zero to positive and negative retrievals, respectively, then calculating the percent of positive retrievals achieved over the 2005-2010 dataset. These calculations were done for CHL only as retrieval frequency for FLH data at NH-10 is assumed to be approximately equal given the application of quality-control flags.

2.3.5 Bloom threshold

A 300% threshold was established to delineate pixel values in bloom product output as representative of "bloom" (greater than 300%) or "non-bloom" (less than 300%) conditions. This threshold isolates the pixels where the most change occurred due to net phytoplankton growth or advection. Nutrient-rich upwelling regimes are typically dominated by diatom blooms, and time series sampling off the central Oregon coast from 2002-2007 shows diatoms indeed dominate annual phytoplankton community composition (unpublished data, courtesy W.T. Peterson). Under the assumption that the relative change observed in product output is due to diatom growth, this threshold can be equated to a phytoplankton specific growth rate (μ) of 0.17 d^{-1} by Equation 2.

$$C_t = C_0 e^{\mu t} \qquad \text{(Equation 2)}$$

Where C_t and C_0 are set equal 3 and 1, respectively, to represent a tripling of chl-a concentration over a time frame, t, of 8 days. This growth rate is reasonably conservative relative to values observed in diatom species common in this region,

which range from approximately 1 to 2 d^{-1} (Kokkinakis & Wheeler 1987, Wetz & Wheeler 2007).

Based on this threshold, daily "bloom indices" were developed to facilitate temporal analysis of blooms detected in regions A-E. For each region, CHL_{dev} and FLH_{dev} bloom indices were derived from the daily percentage of pixels above the bloom threshold relative to the number of total positive retrievals in the region. This ratio was calculated and plotted in time, represented by the final day of the current composite, for each of the five regions spanning 2005-2010. The resulting CHL_{dev} and FLH_{dev} indices describe the spatial extent of potential bloom events detected by the bloom products in each region and enable comparison of bloom product output to time series *in situ* observations. The percent of positive retrievals, i.e. satellite coverage, achieved in the region affects the magnitude of peaks in the indices, hence was also calculated as a coincident proxy of regional spatial coverage. Bloom indices were developed as a temporal metric of bloom events observed by CHL_{dev} and FLH_{dev} instead of daily regional averages of product output as spatial variation would dampen observed bloom signals if the values were averaged across the entire spatial domain.

2.3.6 Evaluation of product performance along the central Oregon coast

The products' ability to detect bloom onset and identify dominant drivers of increased biomass was evaluated in region C through comparison of CHL_{dev} and FLH_{dev} bloom indices to *in situ* metrics of biological and physical parameters. To qualitatively relate bloom events observed via satellite with *in situ* conditions, time series of the satellite indices were plotted with *in situ* temperature, salinity, river discharge and wind stress for May 2009 through April 2010 and highlighted according to wind stress conditions. Upwelling-, downwelling-, or relaxation-favorable conditions were defined as 4 or more days of wind stress values that were predominantly negative (southward), positive (northward), or between ±0.05 N m^2, respectively.

Seasonal cross-correlation analysis was employed to quantify the degree to which bloom onset observed in the indices was correlated with in-water conditions. Prior to analysis, all data were separated into two six-month periods to account for seasonality in primary productivity, wind stress patterns and river discharge: November through April, or winter-spring phase, and May through October, or summer-fall phase, referred to hereafter as "winter" and "summer," respectively. Bloom indices were compared to each other, as well as wind stress, temperature and river discharge.

2.4 Results

2.4.1 Assessments of ocean color products and in situ *variability*

Regressions of daily CHL and FLH against mean daily *in situ* fluorescence at NH-10 yielded r^2 values of 0.36 and 0.61, respectively (Figure 2-2). Both regressions are significant at the $\alpha=0.05$ ($p < 0.0001$) significance level. Decorrelation scales observed in fluorescence data at NH-10 ranged from 3 to 8 days (Figure 2-3b,d,f). Dominant scales were defined as the lag value closest to the 99% significance level.

The average number of consecutive days between positive retrievals, or the average data gap at NH-10, is 4.81 days with a standard deviation of 4.80 days. The distribution is skewed towards zero with a median of 3 days and a mode of 1 day; 75% and 90% of the time data gaps were between 1 to 7 and 1 to 11 days, respectively. Coupled with the observed 3 to 8 day decorrelation scales of biological variability, these results indicate that an 8-day time frame will function as an appropriate length of time for averaging of the current ($\overline{X}_{current}$) and reference ($\overline{X}_{reference}$) composites. This time frame lies approximately in the middle of where these ranges overlap and is also a standard time window for NASA ocean color products.

Annual coverage of daily MODIS CHL data (Figure 2-4a) shows the percent of positive retrievals increases from approximately 25 to 35% along the Oregon coast from north to south. From east to west offshore, coverage decreases with valid

retrievals, declining to approximately 15-20% in the westernmost regions. Coverage at the pixel coincident with NH-10 averages 29%, which lies in the middle of the alongshore range. Considering 29% valid retrievals, 8-day composites permit, on average, a minimum of two retrievals for any nearby pixels over the 8-day time frame.

Mean annual outflow from coastal rivers in regions B-E increases coast-wide approximately November 1st and remains elevated through April, tapering to varying degrees through June and July (Figure 2-1b). Regions D and E have greater average outflow than regions B and C because their rivers represent drainage basins approximately 5 times larger. Columbia River outflow (Figure 2-1b, Region A) is an order of magnitude greater than the average outflow of the coastal rivers in regions B through E due to its significantly larger drainage basin, which spans portions of Montana, Idaho, British Columbia (southwest Canada), Washington and Oregon. Maximum Columbia River outflow is associated with rainfall and spring snowmelt freshets in winter and late spring/early summer, respectively (Hickey 1998). Peaks in coastal river outflow are determined by episodic rainfall events with a frequency of 1-3 times per month in winter through spring (Colbert & McManus 2003, Wetz et al. 2006). In all regions, river outflow minima occur between July and September.

2.4.2 Bloom product imagery

Application of equation 1 derives daily bloom products (e.g. Figure 2-5c, f) from relative differences between successive 8-day "current" and "reference" composites (e.g. Figure 2-5a,b,d,e). Modified anomaly coloration is applied to bloom product imagery, with positive relative differences in shades of red and negative differences in shades of blue. Greater color intensity indicates greater relative percent change in the product. White indicates pixels lacking data due to quality-control flags. Spatial coverage of daily bloom products is determined by the positive retrievals in common between each day's respective current and reference composites. Primary sources of product error include the aforementioned sources of error for standard CHL

and FLH products, composite-averaging of data and spatial coverage of daily CHL and FLH.

Annual coverage of CHL_{dev} for 2005-2010 ranged from approximately 60-80% alongshore from north to south and 40-50% offshore (Figure 2-4b). The pixel coincident with NH-10 had coverage over 76% of the time record. Spatially, coverage is degraded year-round in offshore waters west of approximately 127º longitude due to persistent cloud cover (Figure 2-4b). Temporal coverage of the coastal regions A through E is highly variable within the 5-year dataset, and is generally lowest winter through spring (Figure 2-6). Percent positive retrievals in all five coastal regions are highly variable throughout the year, with the most variability and decreased coverage evident October through May or April, depending on the region (Figure 2-6). Consistent with nearshore spatial trends in standard and bloom product coverage (Figure 2-4), negative retrievals are highest in the north and successively decrease towards the south (Figure 2-6).

Figure 2-9 depicts regional CHL_{dev} and FLH_{dev} bloom index values for May 2009 through winter 2010. Typical patterns observed in all years' data are visible in this figure: higher variability and less coherence between products in winter; signals observed at approximately the same time across several regions, indicating the alongshore extent of bloom events; and, more infrequently, lone peaks in CHL_{dev} or FLH_{dev}.

2.4.3 Product evaluation: A case study of the central Oregon Coast

Time series plots of coincident central coast parameters (Figure 2-10) suggest significant correlation between wind stress, temperature and bloom events during summer months. Seasonal correlation analysis between *in situ* parameters and the bloom indices (Figure 2-11) verify correlation and are summarized in Table 2-1. Dominant temporal decorrelation scales were defined as the lag value closest to the 99% significance level. Cross-correlation results were considered significant if plots exhibited distinctive peaks with minima or maxima above the 99% significance level

(e.g. results shown in Figure 2-11a,c,d) and lag values were less than the decorrelation scales (Table 2-1) associated with the two cross-correlated variables.

Bloom events are evident as well-defined, or successive series of, peaks in the bloom indices. Negative (upwelling), positive (downwelling) or neutral wind stress conditions, highlighted by grey, white and striped bars, respectively, in Figure 2-10, were a primary factor in identification of bloom events. Coincident temperature, salinity, river outflow and an 8-day running spatial average of CHL and FLH values across region C were also used to distinguish the time frame of blooms. In evaluating these data we also note that peak shape and magnitude can be influenced by the regional percentage of positive satellite retrievals. In particular, winter experiences the most frequent periods of low retrievals, hence shows highest variability in the bloom indices (Figure 2-6 and 2-10a,b). Furthermore, as highlighted in Figure 2-10, wind events span several days to weeks, but daily-scale variability is also evident in wind stress and the subsequent biological/physical response within these highlighted regions. For example, the second upwelling event in early June through July of 2009 depicts the onset of upwelling conditions, followed by weakening and onset of high-magnitude downwelling conditions (Figure 2-10d). This daily-scale variability in wind is reflected extremely well in temperature and salinity values (Figure 2-10c), and bloom indices as well-formed peaks (Figure 2-10a,b) associated with high-magnitude upwelling (Figure 2-10d).

Throughout the summer, wind stress conditions were predominantly upwelling-favorable (solid grey regions in Figure 2-10) and coincident with cooling temperatures and increasing salinity, a hallmark of wind-induced upwelling of colder, more saline waters to the surface. Subsequent bloom events described by the CHL_{dev} and FLH_{dev} indices are significantly correlated with wind stress at a lag of +2 ($r=-0.25$ and -0.41, respectively) days, as well as temperature at a lag of -1 ($r=0.41$) and 0 ($r=-0.45$) days (Figure 2-11c,d; Table 2-1), respectively. Major bloom events were detected by both indices ($r=0.58$) with FLH_{dev} leading CHL_{dev} by one day (Figure 2-11a). Transitions from upwelling to downwelling or neutral conditions coincide with

warming and slight freshening, likely due to advection of offshore waters coastward as upwelling relaxes or reverses. Salinity is most variable from late March through June and is attributable to a combination of variable winds and large pulses of fresh water from coastal rivers. No correlation was observed between the bloom product and riverine discharge during the summer; the latter remained at a fairly constant, low volume.

Winter months were dominated by strong, highly variable downwelling-favorable wind events (white regions in Figure 2-10) separated by relaxation events (striped grey regions in Figure 2-10). No significant correlations were observed between either bloom index and wind stress, temperature, or river outflow, nor were the indices correlated with each other. While river discharge and the CHL_{dev} index are potentially correlated (r=0.32) at a lag of 11 days (Figure 2-11f), the lag is outside the variable's respective 2 and 6 day decorrelation scales (Table 2-1). As a result, this relation was considered insignificant (Table 2-1) as it may be attributable to autocorrelation rather than correlation between the two time series. Temperature became progressively cooler November through December then stabilized. Salinity remained relatively consistent throughout winter, except for intermittent pulses of fresher waters associated with neutral or weak downwelling conditions, likely allowing pooling of buoyant freshwater from coastal rivers on top of denser marine waters

2.5 Discussion

2.5.1 Product development

Linear regression of coincident satellite retrievals and *in situ* fluorescence provides a measure of product accuracy and a baseline for inter-comparison of CHL and FLH retrievals. Mooring observations at NH-10 and coincident pixel retrievals are both measured in an Eulerian frame of reference, meaning chl-a and fluorescence variability at a given location are due to growth, decay and advection of surface

blooms. As such, the *in situ* NH-10 records are a reasonable first-order approximation of expected chl-a concentrations and scales of variability that would be observed if daily satellite retrievals at the pixel coincident with NH-10 approached 100%. Relative to CHL, FLH explained nearly twice the *in situ* variance (36%, 61%, respectively; Figure 2-2). This result supports the interpretation of FLH as a indicator of phytoplankton biomass despite the known impact of variable physiology on this product (Behrenfeld et al. 2009). The weaker relationship observed between CHL and *in situ* data may be a consequence of known degradation of CHL algorithm performance in coastal regions due to periodically high concentrations of CDOM which contaminates CHL measurements (Claustre 2003, Siegel et al. 2005a, Werdell et al. 2007). While we have only evaluated the goodness-of-fit for data records immediately around the NH-10 mooring, our results indicate daily L3 MODIS CHL and FLH products processed with the selected application of quality-control flags are a sound foundation for detection of phytoplankton blooms.

Scales of biological variability and satellite data frequency were the primary guiding factors in determining the 8-day time frame of the running current and reference composites that comprise the bloom product algorithm. Observed temporal decorrelation scales in NH-10 fluorescence ranged from 3 to 8 days (Figure 2-3), which is similar to previous studies reporting *in situ* decorrelation scales in the northern CCS: 2.5 days (Abbott and Letelier, 1998) and less than 4.5 days (Frolov et al. in prep), according to chl-a measurements collected via drifter and mooring, respectively.

2.5.2 Trends in bloom product imagery interpretation

Where CHL and FLH describe mesoscale distribution of surface phytoplankton standing stock in terms of bulk chl-a concentration, corresponding CHL_{dev} and FLH_{dev} products describe variability in concentration over time, targeting the growth phase or advective transport of nascent phytoplankton blooms. Daily bloom products depict the relative change observed between successive “current” and “reference” 8-day

composites. The products are influenced by 16 total days of satellite observations and normalized to the "initial" conditions observed during that time frame. Normalization and the relatively short time window removes seasonal influence from the product signal, as seen by the lack of a clear seasonal pattern in the magnitude of the bloom products (Figure 2-9). Satellite coverage of standard CHL and FLH products (Figure 2-4a) influences accuracy of the bloom products as reduced coverage provides fewer data points for composite-averaging. Optimal bloom product coverage, hence greatest accuracy, occurs alongshore (Figure 2-4b) and during months of highest productivity (Figure 2-6). While compositing can dampen observed variability at temporal scales less than 8 days, *in situ* fluorescence (Figure 2-3b,d,f) and temperature (Table 2-1) decorrelation scales indicate that 8-day running composites are sufficient to capture changes in phytoplankton biomass, yet still contain valuable information regarding shorter-term mesoscale variability on the order of weeks to months (Haury et al. 1978, O'Reilly et al. 1998).

CHL and FLH are both adequate proxies of *in situ* chl-a concentration (Figure 2-2), however each are unique in their sources of error. For example, high CDOM loads may lead to overestimates in CHL but should not impact FLH, and physiological changes may impact FLH but not CHL. Considering this, similar spatial patterns and magnitudes of positive relative change observed in coincident CHL_{dev} and FLH_{dev} imagery, or convergent signals, strongly suggest growth or advection of phytoplankton as we cannot conceive of any other processes that would generate positive change in both CHL and FLH. These convergent signals are most commonly observed alongshore as a result of summer upwelling events. For instance, figures 2-5c and 2-5f depict an upwelling event and exhibit convergent patterns of alongshore relative change. Divergent positive signals, i.e. positive relative change of dissimilar magnitude, are typically associated with offshore mesoscale circulation features that induce advective transport of upwelling and riverine material. For example, divergence associated with an apparent mesoscale eddy feature in the southern portion of Figures 2-5c and 2-5f. Divergent signals potentially indicate CHL that is not

associated with active photosynthesis, or contamination of the CHL signal by CDOM. Coincident AVISO SSH anomaly contours for Figure 2-5c (Figure 2-8) add support to these observations. Decreased alongshore SSH anomalies aligned with the coast are indicative of upwelling, supporting the notion that the convergent alongshore signals indicate an upwelling-induced bloom. Concentric positive and negative SSH anomalies show the divergences are associated with advection of particles by velocity fields induced by cyclonic and anticyclonic eddy formations, suggesting the feature represents an older, senescent bloom that has been advected offshore. Figure 2-9 shows these convergences and divergences are also observable in the bloom indices in regions A-C (upwelling) and D-E (eddy circulation).

Strong bloom signals in CHL_{dev} relative to FLH_{dev} that are associated with regions of high-volume freshwater input represent a second example of divergent patterns commonly observed in bloom imagery. For example, Figure 2-7a and 2-7b show divergent signals near the Columbia River mouth and the Juan de Fuca eddy, which has inflow from the Juan de Fuca straight. Pairing the products with coincident SST imagery (Figure 2-7c) shows the regions of divergence are associated with regions of warmer SST near points of freshwater discharge, which is indicative of freshwater intrusions. These product divergences support the assertion that CDOM absorption is likely a source of overestimates in chl-a concentration by CHL retrievals. While this is a limitation in CHL_{dev} accuracy in terms of detection of active phytoplankton blooms, it may prove advantageous as a way to remotely distinguish surges in freshwater outflow from phytoplankton blooms. Product output, including causal factors of bloom signal convergence and divergence, can be verified in more detail using a combination of biological and meterological data available along the Newport hydrographic line.

2.5.3 Product evaluation: A case study of the central Oregon Coast

The observed seasonal and intra-seasonal variability in region C indices and *in situ* biological/physical parameters can be summarized as follows (Figure 2-10). In

summer, coastal river flow is significantly reduced, standing stocks of chl-a are elevated, and predominantly upwelling-favorable winds are interspersed with reversal and relaxation events (Figure 2-10). Peaks in bloom indices are coincident with cooler temperatures and increased salinity, with the exception of bloom activity in October that began during a neutral-phase and warmer temperatures. Winter is characterized by high coastal river outflow, low standing stocks of chl-a and dominated by strong downwelling conditions separated by periods of neutral conditions (Figure 2-10). Peaks in bloom indices are associated with reversals or relaxation of downwelling-favorable winds and show more variability and less coincidence than summer months. River outflow for this time frame is consistent with annual patterns (Figure 2-1b) and the observed biophysical trends are consistent with typical seasonal oceanographic conditions.

The bloom indices performed well in Oregon's central coast waters during summer months when standing stocks of chl-a, and presumably primary productivity, were highest. Five upwelling events occurred during the summer of 2009, and each were followed by a clear biological response in both bloom indices (Figure 2-10). *In situ* fluorescence data spanned four of these events (Figure 2-3e) and confirms the bloom activity detected by both CHL_{dev} and FLH_{dev} (Figure 2-10a,b). Low temperatures and negative wind stresses were followed by peaks in the bloom indices at lags ranging from 0 to +2 days (Figure 2-11c,d; Table 2-1), indicating rapid response of the biology to upwelling-favorable conditions. The CHL_{dev} and FLH_{dev} indices were significantly correlated with each other at a lag of 1 day, meaning bloom events are typically detected by both indices at roughly the same time scales (Figure 2-11a; Table 2-1). Temporal decorrelation scales of bloom indices (5 to 7 days) correspond well with scales of *in situ* temperature and fluorescence (6 and 3 to 8 days, respectively) indicating products have sufficient coverage to capture the region's biological variability in summer months.

In contrast to the summer phase, river discharge and relaxation or reversal of downwelling-favorable winds are likely to affect bloom signals during winter, but no

significant correlations were observed between the indices and *in situ* physical parameters. Percent coverage, and hence accuracy, is reduced during this time of the year (Figure 2-9) and no *in situ* fluorescence data were available to assist evaluation of the bloom indices. Prevalent coastal river outflow in winter (Figure 2-1b) likely fuels significant winter productivity (Wetz et al. 2006) and has strong potential to affect CHL accuracy through CDOM loading (Siegel et al. 2005b). However, limited satellite and *in situ* data coverage confounded determination of whether bloom signals were indicative of CDOM, winter productivity or otherwise. This underscores the importance of enhancing autonomous data collection efforts throughout winter and spring months, including addition of a CDOM fluorometer to the suite of instrumentation on the NH-10 mooring.

Compared to smaller coastal rivers, Columbia River outflow is an order of magnitude larger (Figure 2-1b) as it represents a far more expansive drainage basin. Unlike coastal rivers, outflow is not a metric of its presence, or plume, in Oregon's coastal waters. Rather, the position and geographical extent of the plume is determined by variations in short-term wind stress and river outflow (Hickey et al. 2005). Like coastal river outflow, the plume's position relative to Oregon's coast is significant to regional bloom dynamics as it can stimulate or suppress phytoplankton blooms. Further research and *in situ* data are necessary to define signals indicative of plume waters in these time series and better assess the impact of freshwater outflow on this region's productivity.

The ability to identify coastal blooms via satellite in tandem with autonomous *in situ* parameters affords descriptors of the physical conditions preceding a bloom event. With this information, inferences as to which algal groups may dominate the algal assemblage, i.e. diatoms or dinoflagellates can be made. For example, in early September 2009, strong peaks in both indices followed a brief upwelling event of cold, nutrient-rich waters (arrow on Figure 2-10). This event was followed by wind relaxation and reversal, a concomitant rise in sea surface temperature, and variable activity in the indices (brackets on Figure 2-10) between October and November.

Considering the physical conditions at the time, the former event would likely be a diatom-dominated assemblage, and the latter dominated by dinoflagellates. *In situ* phytoplankton community counts collected along the NH line confirm a diatom bloom was indeed observed in late September (following upwelling) along with the peak in the indices (arrow on Figure 2-10). The subsequent transition to neutral or downwelling-favorable winds and variable activity in the indices (brackets on Figure 2-10) coincided with a significant dinoflagellate bloom of the HAB species *Akashiwo sanguinea* that persisted through early November (Du et al. 2011).

2.6 Conclusion and future direction

This study has shown that the relative change of CHL and FLH can be used to identify the onset of phytoplankton blooms, potentially diagnose CDOM intrusions, and, when viewed in parallel with satellite altimetry, show enhancement or transport of phytoplankton biomass via mesoscale features. Variability is the norm in this region, as evidenced by daily to weekly change in nearly every *in situ* biophysical parameter employed in this research. This fact combined with pervasive cloud cover underscores the difficulty of quantifying bloom events via satellite. However the bloom products were shown to provide sufficient spatial coverage for Oregon's coastal regions and to accurately detect blooms in central coast waters during productive summer and autumn months. In concert with *in situ* data, these products provide a potentially powerful platform for remote identification and monitoring of phytoplankton blooms in response to physical and chemical forcing (e.g. riverine input, wind-driven upwelling). The products we have developed target the critical initiation phase of potential phytoplankton blooms allowing consideration of the mechanisms that trigger blooms and, in combination with maps of absolute concentrations, they can be used to evaluate bloom persistence. Negative indices can also be used to consider the process of bloom decay. If combined with a thorough assessment of the temporal and spatial coverage of the region (as we have done

herein), these products should be useful in other regions to address the phenology of phytoplankton growth, succession patterns and biological/physical coupling.

2.7 Literature cited

Banas N, MacCready P, Hickey B (2009) The Columbia River plume as cross-shelf exporter and along-coast barrier. Continental Shelf Research 29:292-301

Bane JM, Spitz YH, Letelier RM, Peterson WT (2007) Jet stream intraseasonal oscillations drive dominant ecosystem variations in Oregon's summertime coastal upwelling system. Proceedings of the National Academy of Sciences 104:13262

Behrenfeld M, O'Malley R, Siegel D, McClain C, Sarmiento J, Feldman G, Milligan A, Falkowski P, Letelier R, Boss E (2006) Climate-driven trends in contemporary ocean productivity. Nature 444:752-755

Behrenfeld MJ, Westberry TK, Boss ES, O'Malley RT, Siegel DA, Wiggert JD, Franz B, McClain C, Feldman G, Doney SC (2009) Satellite-detected fluorescence reveals global physiology of ocean phytoplankton. Biogeosciences 6:779-794

Claustre H (2003) Ocean Science: The many shades of ocean blue. Science 302:1514-1515

Colbert D, McManus J (2003) Nutrient biogeochemistry in an upwelling-influenced estuary of the Pacific Northwest (Tillamook Bay, Oregon, USA). Estuaries and Coasts 26:1205-1219

Du X, Peterson W, McCulloch A, Liu G (2011) An unusual bloom of the dinoflagellate *Akashiwo sanguinea* off the central Oregon, USA, coast in autumn 2009. Harmful Algae 10:784-793

Evans W, Hales B, Strutton PG (2011) Seasonal cycle of surface ocean pCO2 on the Oregon shelf. Journal of Geophysical Research 116:C05012

Frolov S, Kudela RM, Ryan J (in prep) Phytoplankton blooms along the U.S. West Coast: scales of variability and implications for monitoring of harmful algal blooms.

Grantham BA, Chan F, Nielsen KJ, Fox DS, Barth JA, Huyer A, Lubchenco J, Menge BA (2004) Upwelling-driven nearshore hypoxia signals ecosystem and oceanographic changes in the northeast Pacific. Nature 429:749-754

Haury L, McGowan J, Wiebe P (1978) Patterns and processes in the time-space scales of plankton distributions. Plenum Press, New York

Henson S, Thomas A (2007a) Phytoplankton scales of variability in the California Current System: 1. Interannual and cross-shelf variability. Journal of Geophysical Research 112:C07017

Henson S, Thomas A (2007b) Phytoplankton scales of variability in the California Current System: 2. Latitudinal variability. Journal of Geophysical Research 112:C07018

Hickey B (1998) Coastal oceanography of western North America from the tip of Baja California to Vancouver Island. The Sea 11:345-393

Hickey B, Geier S, Kachel N, MacFadyen A (2005) A bi-directional river plume: The Columbia in summer. Continental Shelf Research 24:1631-1656

Hoge F, Lyon P, Swift R, Yungel J, Abbott M, Letelier R, Esaias W (2003) Validation of Terra-MODIS phytoplankton chlorophyll fluorescence line height: I. Initial airborne lidar results. Applied Ocean Optics 42:2767-2771

Kiefer DA, Reynolds RA (1992) Advances in understanding phytoplankton fluorescence and photosynthesis. Plenum Press, New York

Kokkinakis SA, Wheeler PA (1987) Nitrogen uptake and phytoplankton growth in coastal upwelling regions. Limnology and Oceanography 32:1112-1123

Kudela RM, Horner-Devine AR, Banas NS, Hickey BM, Peterson TD, McCabe RM, Lessard EJ, Frame E, Bruland KW, Jay DA (2010) Multiple trophic levels fueled by recirculation in the Columbia River plume. Geophysical Research Letters 37:L18607

Large W, Pond S (1981) Open ocean momentum flux measurements in moderate to strong winds. Journal of Physical Oceanography 11:324–336

Letelier RM, Abbott MR (1996) An analysis of chlorophyll fluorescence algorithms for the Moderate Resolution Imaging Spectrometer (MODIS). Remote Sensing of Environment 58:215-223

Mieruch S, Freund J, Feudel U, Boersma M, Janisch S, Wiltshire K (2010) A new method of describing phytoplankton blooms: Examples from Helgoland Roads. Journal of Marine Systems 79:36-43

Naik PK, Jay DA (2005) Estimation of Columbia River virgin flow: 1879 to 1928. Hydrological processes 19:1807-1824

O'Reilly JE, Maritorena S, Mitchell BG, Siegel DA, Carder KL, Garver SA, Kahru M, McClain C (1998) Ocean color chlorophyll algorithms for SeaWiFS. Journal of Geophysical Research 103:24937

Phillips EM, Zamon JE, Nevins HM, Gibble CM, Duerr RS, Kerr LH (2011) Summary of birds killed by a harmful algal bloom along the south Washington and north Oregon coasts during October 2009. Northwestern Naturalist 92:120-126

Siegel D, Doney S, Yoder J (2002a) The North Atlantic spring phytoplankton bloom and Sverdrup's critical depth hypothesis. Science 296:730-733

Siegel D, Maritorena S, Nelson N, Behrenfeld M, McClain C (2005a) Colored dissolved organic matter and its influence on the satellite-based characterization of the ocean biosphere. Geophysical Research Letters 32:L20605

Siegel D, Maritorena S, Nelson N, Hansell D, Lorenzi-Kayser M (2002b) Global distribution and dynamics of colored dissolved and detrital organic materials. Journal of Geophysical Research 107:2338

Siegel DA, Maritorena S, Nelson NB, Behrenfeld MJ, McClain CR (2005b) Colored dissolved organic matter and its influence on the satellite-based characterization of the ocean biosphere. Geophysical Research Letters 32:L20605

Smayda TJ (1997a) Harmful algal blooms: their ecophysiology and general relevance to phytoplankton blooms in the sea. Limnology and Oceanography 42:1137-1153

Smayda TJ (1997b) What is a bloom? A commentary. Limnology and Oceanography 42:1132-1136

Stumpf RP (2001) Applications of satellite ocean color sensors for monitoring and predicting harmful algal blooms. Human and Ecological Risk Assessment 7:1363-1368

Trainer VL, Pitcher GC, Reguera B, Smayda TJ (2010) The distribution and impacts of harmful algal bloom species in eastern boundary upwelling systems. Progress in Oceanography 85:33-52

Tweddle JF, Strutton PG, Foley DG, O'Higgins L, Wood AM, Scott B, Everroad RC, Peterson WT, Cannon D, Hunter M, Forster Z (2010) Satellite phenology of coastal Oregon upwelling and phytoplankton blooms: Relationship to phycotoxins in coastal shellfish. Marine Ecology Progress Series 405:131-145

Venegas R, Strub P, Beier E, Letelier R, Thomas A, Cowles T, James C, Soto-Mardones L, Cabrera C (2008) Satellite-derived variability in chlorophyll, wind stress, sea surface height, and temperature in the northern California Current System. Journal of Geophysical Research 113:C03015

Ware DM, Thomson RE (1991) Link between long-term variability in upwelling and fish production in the northeast Pacific Ocean. Canadian Journal of Fisheries and Aquatic Sciences 48:2296-2306

Ware DM, Thomson RE (2005) Bottom-up ecosystem trophic dynamics determine fish production in the Northeast Pacific. Science 308:1280

Werdell P, Bailey S (2005) An improved in-situ bio-optical data set for ocean color algorithm development and satellite data product validation. Remote Sensing of Environment 98:122-140

Werdell P, Franz B, Bailey S, Harding L, Feldman G (2007) Approach for the long-term spatial and temporal evaluation of ocean color satellite data products in a coastal environment In: Frouin, RJ (ed) Coastal Ocean Remote Sensing Proceedings of SPIE, p 66800G

Wetz M, Hales B, Chase Z, Wheeler P, Whitney M (2006) Riverine input of macronutrients, iron, and organic matter to the coastal ocean off Oregon, USA, during the winter. Limnology and Oceanography 51:2221-2231

Wetz MS, Wheeler PA (2007) Release of dissolved organic matter by coastal diatoms. Limnology and Oceanography 52:798-807

Wilson C (2003) Late summer chlorophyll blooms in the oligotrophic North Pacific Subtropical Gyre. Geophysical Research Letters 30:1942

		--Auto Corr--	------ Cross Correlation -----	
			CHL_{dev}	FLH_{dev}
Summer/Autumn	CHL_{dev}	+/- 5	-	-1 (0.58)
	FLH_{dev}	+/- 7	-	-
	Temperature	+/- 6	-1 (-0.41)	0 (-0.45)
	Wind Stress	+/- 2	+2 (-0.25)	+2(-0.41)
	River Discharge	NS	NS	NS
Winter/Spring	CHL_{dev}	+/- 2	-	NS
	FLH_{dev}	+/- 5	-	-
	Temperature	NS	NS	NS
	Wind Stress	+/- 1	NS	NS
	River Discharge	+/-6	NS	NS

Table 2-1: Temporal lags and correlation coefficients (delineated by parenthesis) between central Oregon coast bloom indices and *in situ* parameters. Time series of parameters (leftmost column) were correlated with themselves (center column) and the CHL_{dev} and FLH_{dev} indices (two rightmost columns). Time series in the rightmost columns follow the time series leftmost column according to the reported lag. For example, in summer/autumn wind stress and the FLH_{dev} index are significantly correlated (r=-0.41) at a lag of +2 days, i.e. the blooms observed by the index most frequently occur two days after peaks in negative (upwelling-favorable) wind stress. Insignificant correlations are indicated by 'NS' and '-' indicates pairings that are not applicable. All correlations reported are above the 99% significance level where n=183 and 182 in summer/fall and winter/spring, respectively.

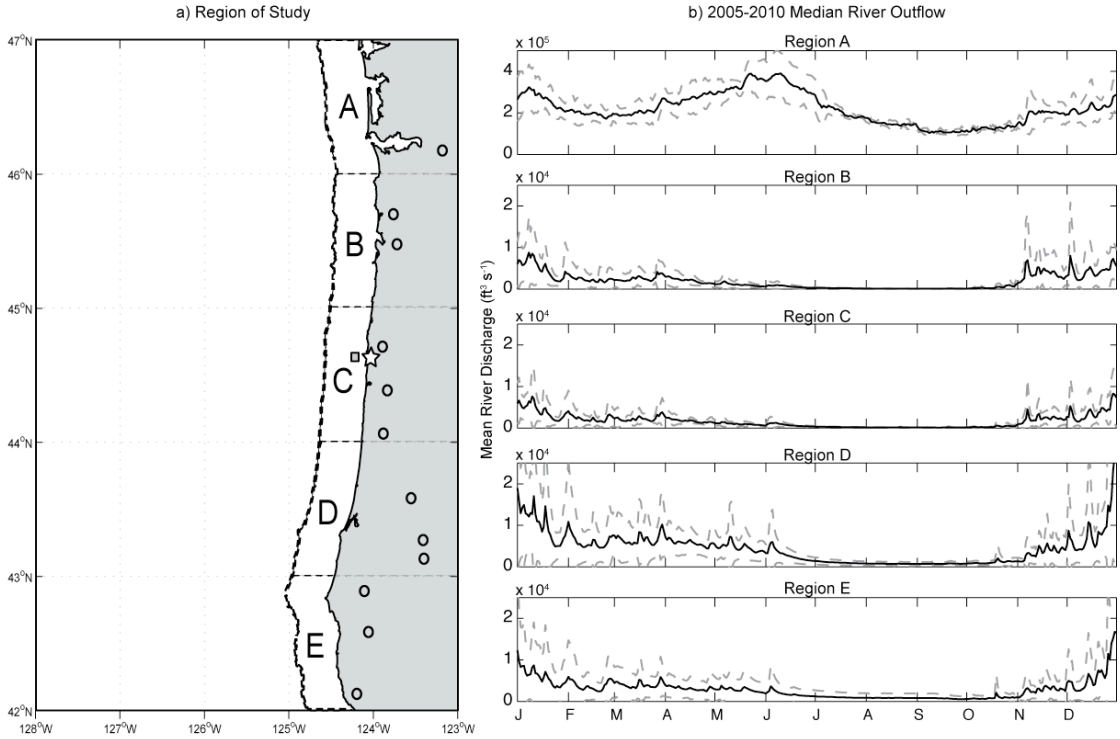

Figure 2-1: Region of study and regional annual river outflow. a) Oregon and southern Washington's coastal waters are defined by regions A through E, which extend 55 kilometers (0.5° longitude) offshore. Circles indicate location of USGS river gauging stations. Star represents Newport, Oregon where wind data were collected. Square indicates location of the NH-10 mooring where *in situ* biological/physical parameters were collected. b) Median annual river outflow (solid black lines) and standard deviation (grey dashed lines) for regions A through E.

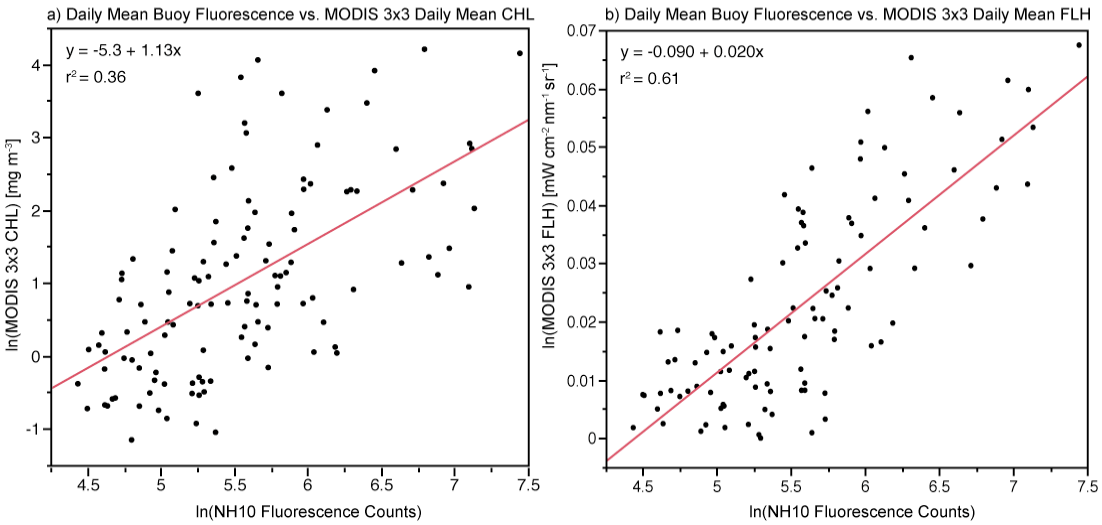

Figure 2-2: Linear regression of daily mean raw fluorescence at the NH-10 mooring and daily mean MODIS a) CHL and b) FLH products. MODIS L3 1KM standard CHL and FLH products were averaged over a 3x3 pixel region centered at NH-10. Linear regression equations and r^2 values are shown for each relationship.

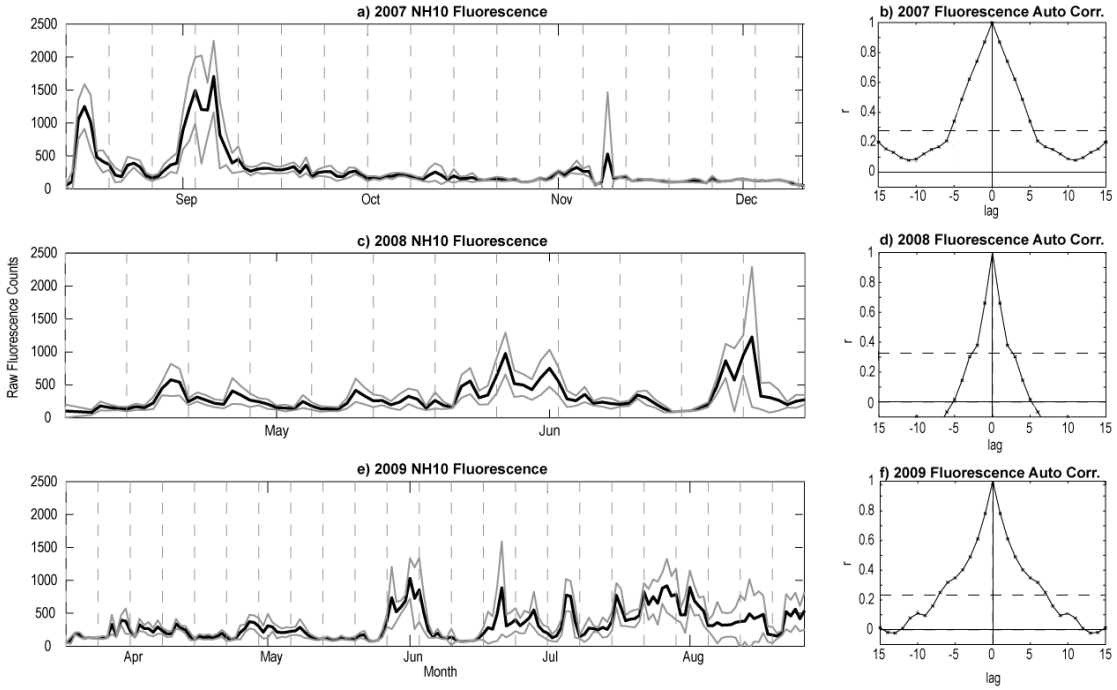

Figure 2-3: Time series of NH-10 mooring fluorescence for a) 2007, c) 2008 and e) 2009 and their respective correlation functions (b, d, f). Black lines in time series are daily average values and solid grey lines represent the standard deviation of the daily averages. Note differences in x axes of plots a, c and e (dashed lines indicate 7-day intervals for scale). Vertical dashed lines on b, d and f indicate 99% significance level.

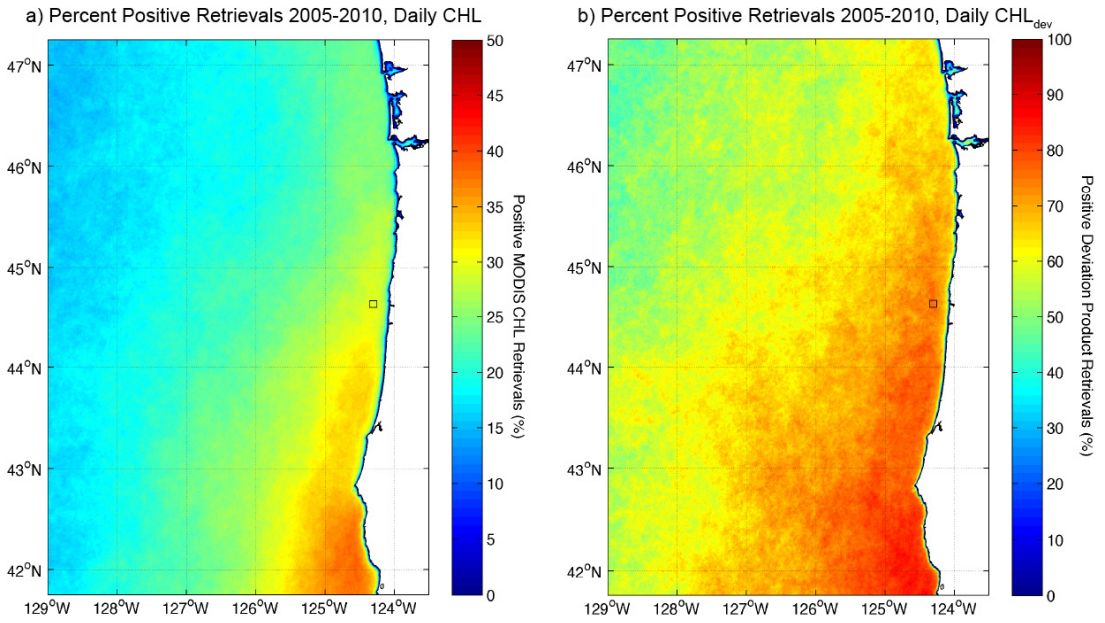

Figure 2-4: Percent positive retrievals off the Oregon and southern Washington coastlines for daily MODIS L3 a) CHL and b) CHL_{dev} from 2005-2010. Note difference in scale. Box indicates location of hydrographic station NH-10.

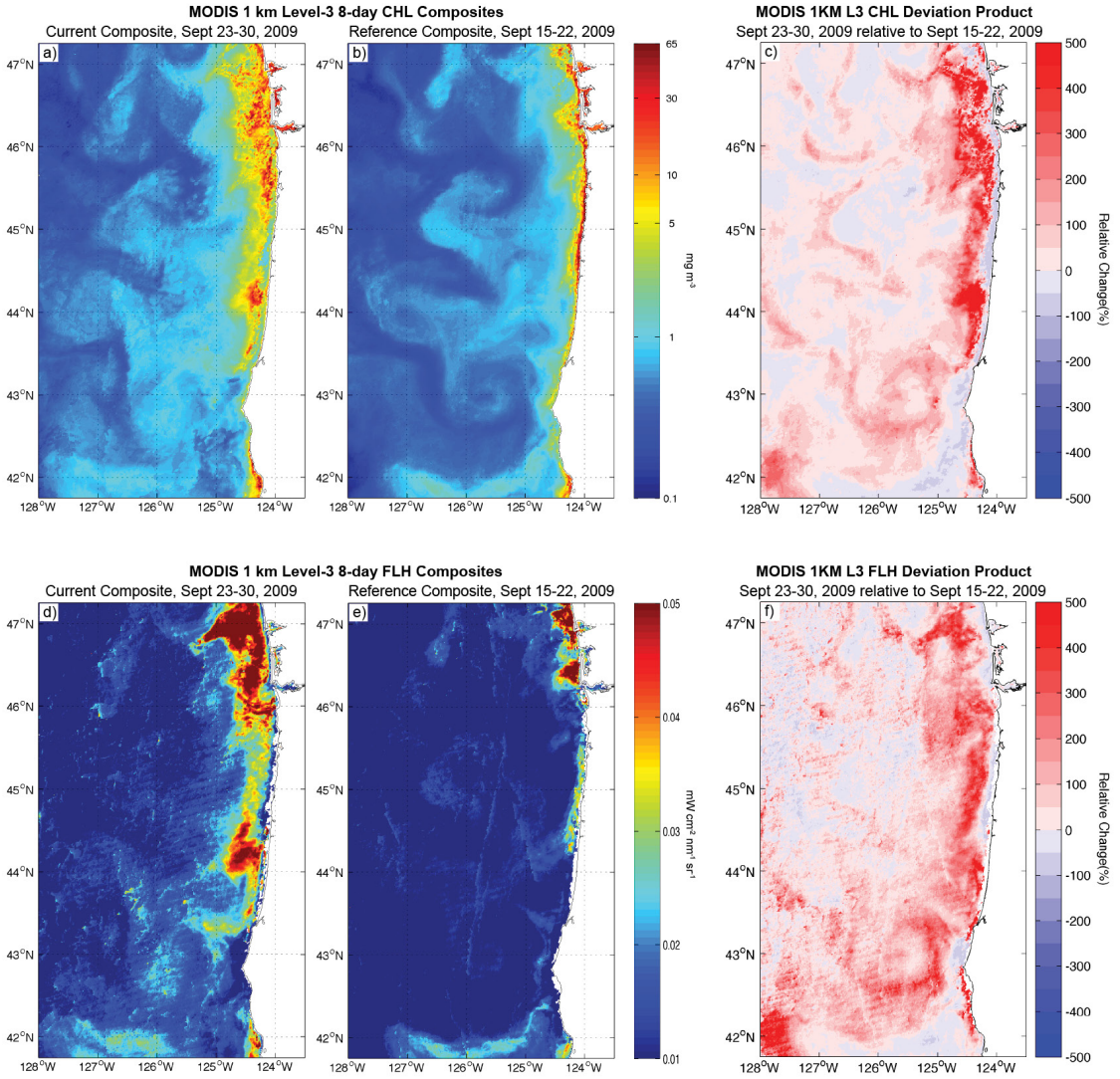

Figure 2-5: Sample of "current" and "reference" 8-day composite imagery for standard CHL (a and b) and FLH (d and e) products. CHL_{dev} and FLH_{dev} imagery (c and f) were created by subtracting the reference from the current composite, then normalizing the result to the reference. CHL_{dev} and FLH_{dev} imagery displays the pixel-by-pixel relative percent change observed in 8-day CHL and FLH over a 16-day time frame. Notable features in c) and f) include convergent alongshore bloom signals (similar positive magnitudes) indicative of an upwelling event, and divergent (dissimilar positive magnitudes) offshore signals associated with mesoscale circulation features.

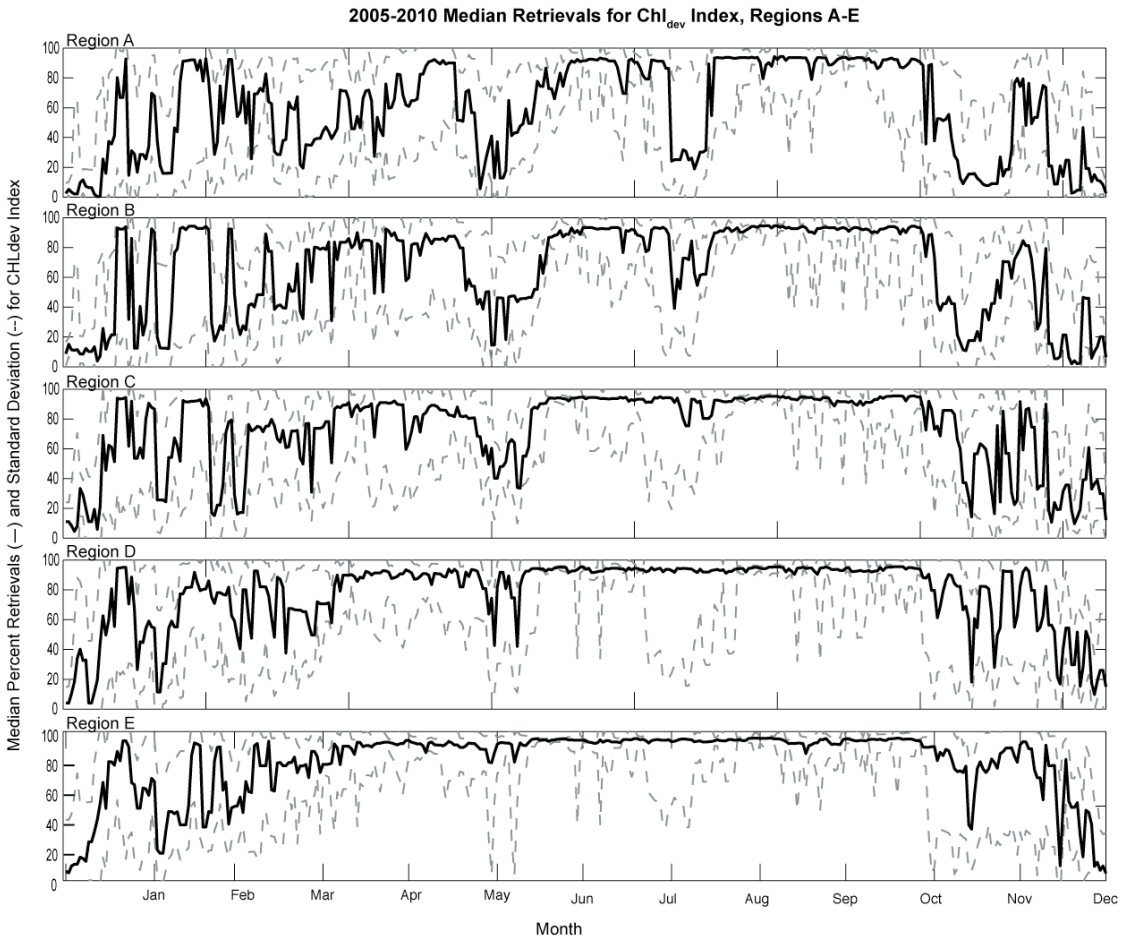

Figure 2-6: Regional median annual retrievals (solid black) and standard deviation (dashed grey) for the CHL_{dev} index, 2005-2010.

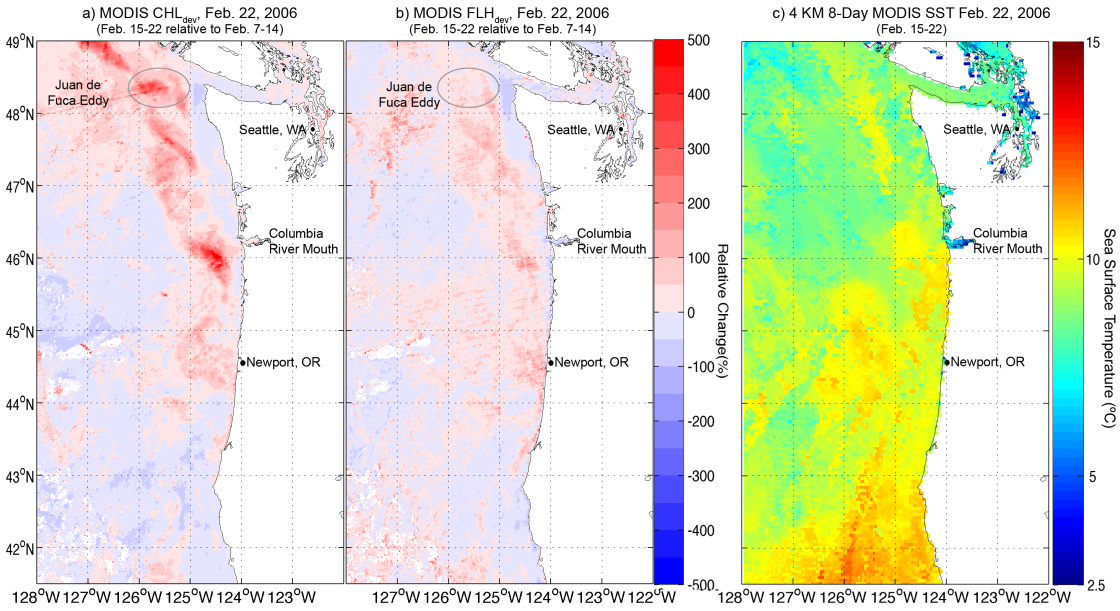

Figure 2-7: Example of divergent bloom product output. Note the stronger signal in a) CHL_{dev} relative to b) FLH_{dev} near the mouth of the Columbia River and offshore of the Washington and Canadian coasts, particularly the Juan de Fuca Eddy. Panel c) shows coincident 4 KM MODIS 8-day SST. Warmer water temperatures are associated with the regions of divergence, supporting the notion that freshwater intrusions induce an apparent bloom signal due to CDOM loading.

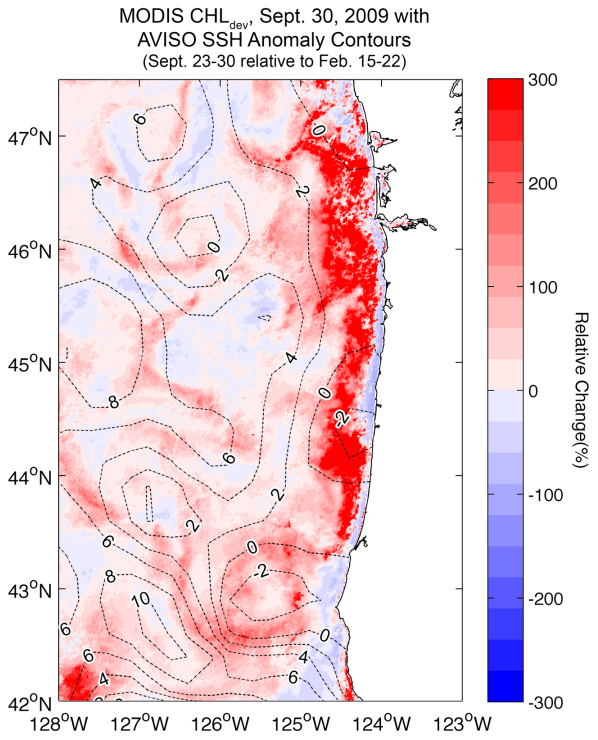

Figure 2-8: CHL_{dev} for September 30, 2009 (i.e. Figure 2-5d) with AVISO sea surface height anomaly contours at 2-centimeter intervals for the week of September 26th, 2009. Regions of strongest bloom signals (i.e. the alongshore convergent signals noted in Figure 2-5d,f) are associated with upwelling and weaker signals (i.e. the offshore divergent signals in Figure 2-5d,f) are associated with advection of blooms offshore by velocity fields associated with eddy formations.

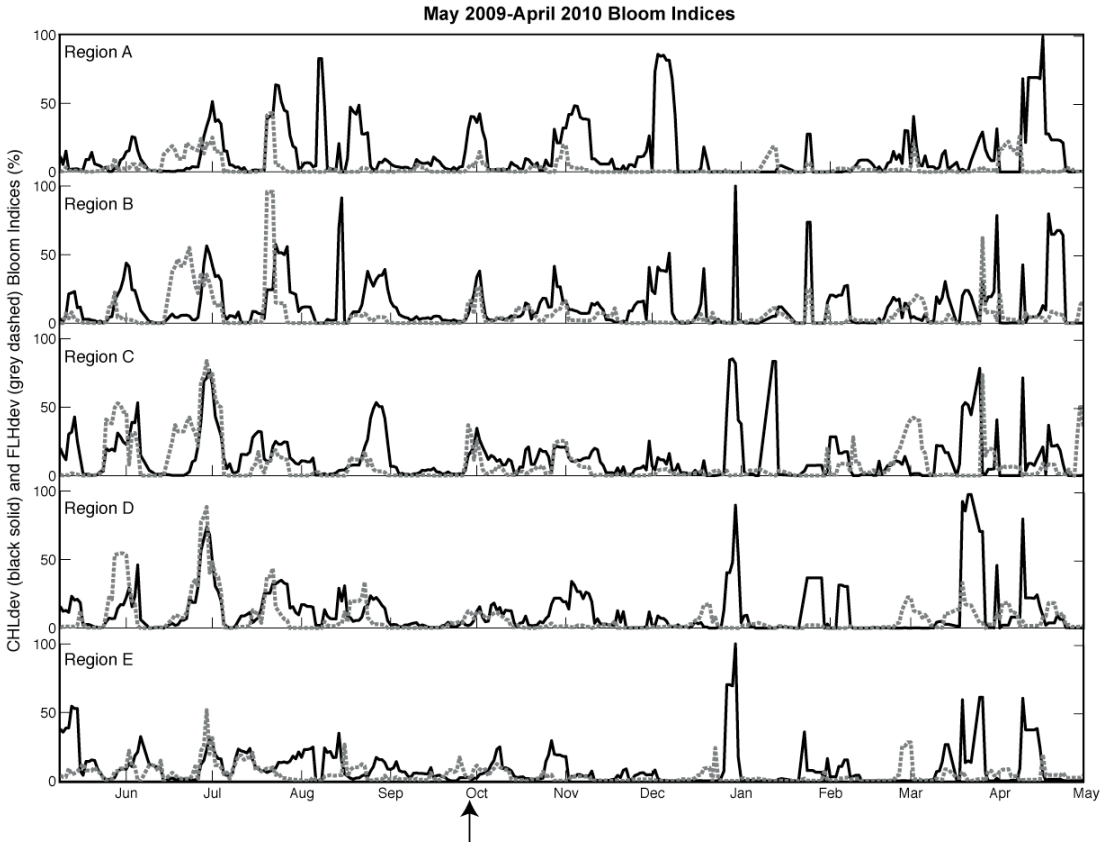

Figure 2-9: Regional CHL_{dev} (solid black) and FLH_{dev} (dashed grey) bloom indices for May 2009 through winter of 2010. Arrow indicates location in time of September 30, 2009 upwelling event (Figure 2-5).

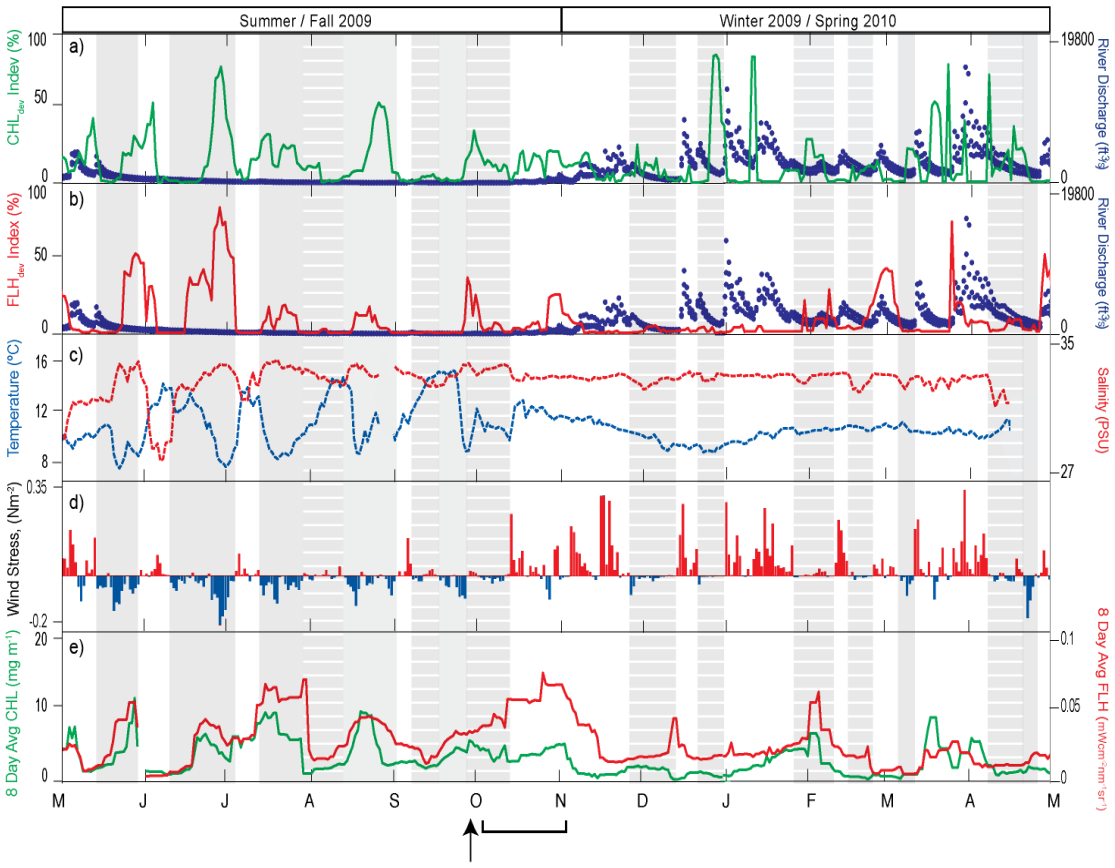

Figure 2-10: Time series data for the central Oregon coast from May 2009 through April 2010: panels a) and b) represent CHL_{dev} and FLH_{dev} bloom indices overlaid on coastal river outflow; c) represents temperature and salinity mooring data at NH-10; d) describes observed winds at Newport, OR; and e) describes spatial CHL and FLH averages for region C derived from running 8-day standard products. Upwelling-, downwelling- and relaxation-favorable winds are highlighted by solid grey, white and striped grey bars, respectively. Summer and winter divisions of time series are indicated by bars at the top. Arrow at bottom indicates location in time of September 30, 2009 upwelling event (Figure 2-5, 2-8); bracket at bottom indicates observed extent of an *Akashiwo sanguinea* bloom in region C.

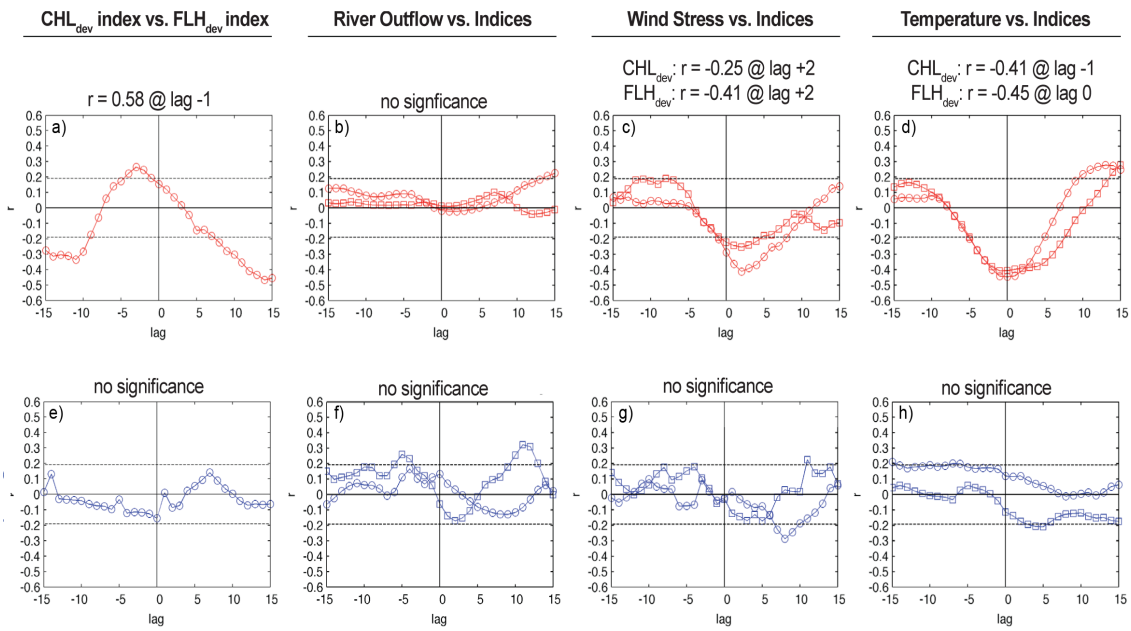

Figure 2-11: Correlation results for the CHL_{dev} index versus the FLH_{dev} bloom index (a and e) and river outflow (b and f), wind stress (c and g), and temperature (d and h) versus the CHL_{dev} (circles) and FLH_{dev} (squares) indices. Plots a, b, c, d represent summer/autumn 2009 (red), and plots e, f, g, h represent winter 2009/spring 2010 (blue). Dashed lines indicate 99% significance level.

3. Conclusions and Future Direction

Phytoplankton comprise the base of the marine food web and are regulators of global biogeochemical cycles. How their abundance and distribution varies over time is vital to determining their roles in the marine biosphere at regional and global scales. The bloom products developed and analyzed herein have shown that the relative change between CHL and FLH biomass effectively identifies nascent blooms in Oregon's coastal waters via satellite. Product indices detect bloom events in time, while daily imagery identifies them in space, providing a way to monitor bloom onset and subsequent advection over time. Similarities and differences in the spatial extent and magnitude of bloom signals observed by coincident bloom products provide more information than either product would alone. Combined with *in situ* and satellite-derived physical proxies, these products have strong potential in research applications off the Oregon coast, as well as regions with similar biophysical dynamics.

The successful development and initial analysis of these products will be followed by evaluation of their utility to identify and monitor harmful algal bloom (HAB) events. The primary HABs of concern in this region include species of toxigenic diatoms and dinoflagellates belonging to the genera *Pseudonitzschia* and *Alexandrium* (Trainer et al. 2010), respectively. Prolonged interaction of toxic HAB events with the shore causes bioaccumulation of phycotoxins in the tissues of filter-feeding shellfish, including razorclams and mussels, leading to closures of commercial and recreational shellfish harvesting (Trainer et al. 2010). The surfactant-producing dinoflagellate *Akashiwo sanguinea* has been identified in recent years as third HAB species of concern for the region (Du et al. 2011). Senescing blooms combined with windy conditions create foam that destroys the insulating capabilities of seabird feathers, causing widespread hypothermia-induced mortality events (Phillips et al. 2011).

Current ocean color sensors do not have the capability to identify algal assemblage composition, hence cannot distinguish HAB blooms from others. However, HAB-forming species can comprise a significant fraction of total

phytoplankton biomass in surface blooms along the Oregon coast. This suggests bulk proxies of chl-a concentration, such as CHL or FLH and their associated bloom products, are potentially useful tools to inform HAB-monitoring efforts. In this regard, time series analysis of the central Oregon coast will be extended to span 2005-2010 and coupled with long-term *in situ* HAB monitoring data obtained by shipboard sampling. Available data include phytoplankton abundance at the genus and species level and hydrographic parameters collected during routine surveys along the central Oregon coast, as well as routine surf-zone biotoxin levels in shellfish tissue. HAB data will be compared to bloom indices and deviation product imagery to assess their effectiveness in identification and monitoring of HAB events.

3.1 Literature cited

Du X, Peterson W, McCulloch A, Liu G (2011) An unusual bloom of the dinoflagellate *Akashiwo sanguinea* off the central Oregon, USA, coast in autumn 2009. Harmful Algae 10:784-793

Phillips EM, Zamon JE, Nevins HM, Gibble CM, Duerr RS, Kerr LH (2011) Summary of birds killed by a harmful algal bloom along the south Washington and north Oregon coasts during October 2009. Northwestern Naturalist 92:120-126

Trainer VL, Pitcher GC, Reguera B, Smayda TJ (2010) The distribution and impacts of harmful algal bloom species in eastern boundary upwelling systems. Progress in Oceanography 85:33-52

4. BIBLIOGRAPHY

Ardanuy PE, Han D, Salomonson VV (1991) The Moderate Resolution Imaging Spectrometer (MODIS) science and data system requirements. Geoscience and Remote Sensing 29:75-88

Banas N, MacCready P, Hickey B (2009) The Columbia River plume as cross-shelf exporter and along-coast barrier. Continental Shelf Research 29:292-301

Bane JM, Spitz YH, Letelier RM, Peterson WT (2007) Jet stream intraseasonal oscillations drive dominant ecosystem variations in Oregon's summertime coastal upwelling system. Proceedings of the National Academy of Sciences 104:13262

Behrenfeld M, O'Malley R, Siegel D, McClain C, Sarmiento J, Feldman G, Milligan A, Falkowski P, Letelier R, Boss E (2006) Climate-driven trends in contemporary ocean productivity. Nature 444:752-755

Behrenfeld MJ, Westberry TK, Boss ES, O'Malley RT, Siegel DA, Wiggert JD, Franz B, McClain C, Feldman G, Doney SC (2009) Satellite-detected fluorescence reveals global physiology of ocean phytoplankton. Biogeosciences 6:779-794

Claustre H (2003) Ocean Science: The many shades of ocean blue. Science 302:1514-1515

Colbert D, McManus J (2003) Nutrient biogeochemistry in an upwelling-influenced estuary of the Pacific Northwest (Tillamook Bay, Oregon, USA). Estuaries and Coasts 26:1205-1219

Du X, Peterson W, McCulloch A, Liu G (2011) An unusual bloom of the dinoflagellate *Akashiwo sanguinea* off the central Oregon, USA, coast in autumn 2009. Harmful Algae 10:784-793

Evans W, Hales B, Strutton PG (2011) Seasonal cycle of surface ocean pCO2 on the Oregon shelf. Journal of Geophysical Research 116:C05012

Frolov S, Kudela RM, Ryan J (in prep) Phytoplankton blooms along the U.S. West Coast: scales of variability and implications for monitoring of harmful algal blooms.

Grantham BA, Chan F, Nielsen KJ, Fox DS, Barth JA, Huyer A, Lubchenco J, Menge BA (2004) Upwelling-driven nearshore hypoxia signals ecosystem and oceanographic changes in the northeast Pacific. Nature 429:749-754

Haury L, McGowan J, Wiebe P (1978) Patterns and processes in the time-space scales of plankton distributions. Plenum Press, New York

Henson S, Thomas A (2007a) Phytoplankton scales of variability in the California Current System: 1. Interannual and cross-shelf variability. Journal of Geophysical Research 112:C07017

Henson S, Thomas A (2007b) Phytoplankton scales of variability in the California Current System: 2. Latitudinal variability. Journal of Geophysical Research 112:C07018

Hickey B (1998) Coastal oceanography of western North America from the tip of Baja California to Vancouver Island. The Sea 11:345-393

Hickey B, Geier S, Kachel N, MacFadyen A (2005) A bi-directional river plume: The Columbia in summer. Continental Shelf Research 24:1631-1656

Hoge F, Lyon P, Swift R, Yungel J, Abbott M, Letelier R, Esaias W (2003) Validation of Terra-MODIS phytoplankton chlorophyll fluorescence line height: I. Initial airborne lidar results. Applied Ocean Optics 42:2767-2771

Hooker S, Esaias W (1993) An overview of the SeaWiFS project. EOS Transactions 74:241-241

Hovis W, Clark D, Anderson F, Austin R, Wilson W, Baker E, Ball D, Gordon H, Mueller J, El-Sayed S (1980) Nimbus-7 Coastal Zone Color Scanner: system description and initial imagery. Science 210:60

Kiefer DA, Reynolds RA (1992) Advances in understanding phytoplankton fluorescence and photosynthesis. Plenum Press, New York

Kokkinakis SA, Wheeler PA (1987) Nitrogen uptake and phytoplankton growth in coastal upwelling regions. Limnology and Oceanography 32:1112-1123

Kudela RM, Horner-Devine AR, Banas NS, Hickey BM, Peterson TD, McCabe RM, Lessard EJ, Frame E, Bruland KW, Jay DA (2010) Multiple trophic levels fueled by recirculation in the Columbia River plume. Geophysical Research Letters 37:L18607

Large W, Pond S (1981) Open ocean momentum flux measurements in moderate to strong winds. Journal of Physical Oceanography 11:324–336

Letelier RM, Abbott MR (1996) An analysis of chlorophyll fluorescence algorithms for the Moderate Resolution Imaging Spectrometer (MODIS). Remote Sensing of Environment 58:215-223

Mieruch S, Freund J, Feudel U, Boersma M, Janisch S, Wiltshire K (2010) A new method of describing phytoplankton blooms: Examples from Helgoland Roads. Journal of Marine Systems 79:36-43

Naik PK, Jay DA (2005) Estimation of Columbia River virgin flow: 1879 to 1928. Hydrological processes 19:1807-1824

O'Reilly JE, Maritorena S, Mitchell BG, Siegel DA, Carder KL, Garver SA, Kahru M, McClain C (1998) Ocean color chlorophyll algorithms for SeaWiFS. Journal of Geophysical Research 103:24937

Phillips EM, Zamon JE, Nevins HM, Gibble CM, Duerr RS, Kerr LH (2011) Summary of birds killed by a harmful algal bloom along the south Washington and north Oregon coasts during October 2009. Northwestern Naturalist 92:120-126

Siegel D, Doney S, Yoder J (2002a) The North Atlantic spring phytoplankton bloom and Sverdrup's critical depth hypothesis. Science 296:730-733

Siegel D, Maritorena S, Nelson N, Behrenfeld M, McClain C (2005a) Colored dissolved organic matter and its influence on the satellite-based characterization of the ocean biosphere. Geophysical Research Letters 32:L20605

Siegel D, Maritorena S, Nelson N, Hansell D, Lorenzi-Kayser M (2002b) Global distribution and dynamics of colored dissolved and detrital organic materials. Journal of Geophysical Research 107:2338

Siegel DA, Maritorena S, Nelson NB, Behrenfeld MJ, McClain CR (2005b) Colored dissolved organic matter and its influence on the satellite-based characterization of the ocean biosphere. Geophysical Research Letters 32:L20605

Smayda TJ (1997a) Harmful algal blooms: their ecophysiology and general relevance to phytoplankton blooms in the sea. Limnology and Oceanography 42:1137-1153

Smayda TJ (1997b) What is a bloom? A commentary. Limnology and Oceanography 42:1132-1136

Stumpf RP (2001) Applications of satellite ocean color sensors for monitoring and predicting harmful algal blooms. Human and Ecological Risk Assessment 7:1363-1368

Trainer VL, Pitcher GC, Reguera B, Smayda TJ (2010) The distribution and impacts of harmful algal bloom species in eastern boundary upwelling systems. Progress in Oceanography 85:33-52

Tweddle JF, Strutton PG, Foley DG, O'Higgins L, Wood AM, Scott B, Everroad RC, Peterson WT, Cannon D, Hunter M, Forster Z (2010) Satellite phenology of coastal Oregon upwelling and phytoplankton blooms: Relationship to phycotoxins in coastal shellfish. Marine Ecology Progress Series 405:131-145

Venegas R, Strub P, Beier E, Letelier R, Thomas A, Cowles T, James C, Soto-Mardones L, Cabrera C (2008) Satellite-derived variability in chlorophyll, wind stress, sea surface height, and temperature in the northern California Current System. Journal of Geophysical Research 113:C03015

Ware DM, Thomson RE (1991) Link between long-term variability in upwelling and fish production in the northeast Pacific Ocean. Canadian Journal of Fisheries and Aquatic Sciences 48:2296-2306

Ware DM, Thomson RE (2005) Bottom-up ecosystem trophic dynamics determine fish production in the Northeast Pacific. Science 308:1280

Werdell P, Bailey S (2005) An improved in-situ bio-optical data set for ocean color algorithm development and satellite data product validation. Remote Sensing of Environment 98:122-140

Werdell P, Franz B, Bailey S, Harding L, Feldman G (2007) Approach for the long-term spatial and temporal evaluation of ocean color satellite data products in a coastal environment In: Frouin, RJ (ed) Coastal Ocean Remote Sensing Proceedings of SPIE, p 66800G

Wetz M, Hales B, Chase Z, Wheeler P, Whitney M (2006) Riverine input of macronutrients, iron, and organic matter to the coastal ocean off Oregon, USA, during the winter. Limnology and Oceanography 51:2221-2231

Wetz MS, Wheeler PA (2007) Release of dissolved organic matter by coastal diatoms. Limnology and Oceanography 52:798-807

Wilson C (2003) Late summer chlorophyll blooms in the oligotrophic North Pacific Subtropical Gyre. Geophysical Research Letters 30:1942